Lack of hyperfine shifts in Doppler-limited spectra of molecular hydrogen

Hubert Jóźwiak [*] and Piotr Wcisło [†]

Institute of Physics, Faculty of Physics, Astronomy and Informatics, Nicolaus Copernicus University in Toruń, Grudziądzka 5, 87-100 Toruń, Poland

(Received 4 November 2022; accepted 9 December 2022; published 3 January 2023)

Accurate spectroscopy of molecular hydrogen isotopologues is used for testing quantum electrodynamics and searching for physics beyond the standard model. Recent measurements of energies of rovibrational resonances in the ground electronic state have reached a level of uncertainty lower than the magnitude of the hyperfine splitting. The underlying hyperfine components of the resonance clearly perturb sub-Doppler saturation spectra. The extent to which hyperfine structure influences the Doppler-limited spectra is not fully understood, as there are two contradicting experimental works that show either a 350 kHz shift or lack of any deviation from the central frequency of the resonance in the HD molecule. Here, we address this problem theoretically. Using the spherical tensor approach, we prove that the barycenter of all hyperfine-resolved spectra corresponds to the unperturbed transition frequency (the first moment of the hyperfine-resolved spectra vanishes). This property is directly transferred to Doppler-limited spectra: we show that there is no detectable shift due to the hyperfine structure unless the ratio of the Doppler width to the root-mean-square hyperfine splitting is less than 50.

DOI: 10.1103/PhysRevA.107.012802

I. INTRODUCTION

Precise spectroscopic studies of simple atomic and molecular systems allow for the performance of accurate tests of quantum theory [1,2], determination of fundamental constants [3,4], and search for physics beyond the standard model [5,6]. Molecular hydrogen, the simplest neutral diatomic molecule, possesses a large number of ultralong-living rovibrational states [7]. The electric dipole transitions between these states are either very weak in heteronuclear isotopologues (HD, HT, and DT) or forbidden in homonuclear isotopologues (H_2, D_2, and T_2). In the latter case, the transitions are electric quadrupole [8] or magnetic dipole [9] in nature. These resonances are extremely narrow—the largest transition probabilities for spontaneous emission in H_2 are of the order of 10^{-6} s^{-1} [10]. The presence of these narrow transitions stimulates accurate spectroscopic measurements in molecular hydrogen and its isotopologues for fundamental studies [11–16]. The most accurate determination of the central frequency of a rovibrational transition in the HD isotopologue has reached the level of 13 kHz, which corresponds to the 0.12 ppb relative uncertainty [11]. Further essential experimental progress requires trapping a cold H_2 sample in either a magnetic trap or an optical dipole trap; the latter seems to be the most promising one as recently a magic wavelength (in infrared) for one of the rovibrational lines was identified in H_2 [17].

The hyperfine structure (HFS) of rovibrational states in molecular hydrogen and its isotopologues has recently gained significant attention from the spectroscopic community [18–25]. Theoretical studies of hyperfine interactions are driven by remarkably accurate experimental studies of the frequencies of rovibrational transitions [11,12,14,26–36] and dissociation energies [37–39]. The importance of the hyperfine structure in the saturation spectra of the 2-0 R(1) transition in HD was recognized by Diouf *et al.* [34], who attributed an outstanding discrepancy between the transition frequencies measured by the Hefei [30] and Amsterdam [31] groups, to crossover resonances between hyperfine components of this line. Hyperfine components of rovibrational transitions should also be carefully analyzed in accurate experiments performed using Doppler-limited spectroscopy [14,28,32,35]. We recall that measurements using cavity-enhanced techniques have achieved the accuracy of 75 kHz [15] for the dipole transition in HD and 117 kHz for the weaker electric quadrupole transition in D_2 [14]. Although unresolved, the hyperfine structure of the R(1) 2-0 line measured by the group in Caserta led to the 350 kHz shift in the determined transition frequency [15]. Since the Doppler width of this transition is, at room temperature, of an order of GHz, it remains an open question whether the hyperfine structure, which spans over the range of hundreds of kHz, could influence the determined transition frequency or whether the inclusion of a large number of components (21) could lead to numerical problems in the fitting procedure. Interestingly, the recent studies, by the group in Grenoble, of the 2-0 R(0) and R(1) lines in HD, performed using Doppler-limited spectroscopy at 80 K, showed no deviation of the apparent line center from the HFS-free transition frequency [40]. The lack of hyperfine shift of the same line, which is almost two times narrower at 80 K than at room temperature, casts a doubt on the conclusions of Ref. [15]. Hence, there is a need for theoretical work that could explain the apparent discrepancy between Refs. [15,40].

The positions and intensities of hyperfine components of dipole and quadrupole transitions in hydrogen isotopologues were recently studied by several authors [18–25]. In particular, the authors of this manuscript reported hyperfine coupling constants, positions and intensities of all rovibrational electric

[*] hubert.jozwiak@doktorant.umk.pl
[†] piotr.wcislo@umk.pl

dipole transitions in HD [19], HT, and DT [24], and electric quadrupole transitions in H_2, D_2 [20], HD [25], and the three tritium-bearing isotopologues [22]. In some cases, hyperfine components seem to be spread almost symmetrically around the central frequency (as in the case of the Q lines), while in others, several blue- or red-detuned components dominate the spectrum. In this work, we analyze theoretically the first moment (the barycenter) of the hyperfine structure of all rovibrational transitions studied in Refs. [19,20,22,24,25]. First, we provide a rigorous proof that the barycenter vanishes for the stick hyperfine spectra (i.e., when each component is an infinitely sharp line). Second, we analyze the first moment of the Doppler-broadened spectra, which is based on a well-known property of Gaussian functions and a discussion of the global maximum of the sum of N-Gaussian functions, which is provided in Appendix D. Finally, we discuss the implication of the results derived here for accurate Doppler-limited measurements of rovibrational transitions in hydrogen isotopologues [14,15,32,40], providing a theoretical input to the discussion about a presence or lack of hyperfine shift in this kind of spectroscopy. This work can also be considered as an extension of our recent analysis of relative intensities of hyperfine components of rovibrational transitions in the six isotopologues of hydrogen [41]. Since the relative intensity can be viewed as the zeroth moment of the hyperfine spectrum, we take this analysis a step further and we study the first moments of this spectrum. Thus, we use the notation introduced in Ref. [41] throughout the article.

II. THE FIRST DISTRIBUTION MOMENT (THE BARYCENTER) OF THE HYPERFINE STICK SPECTRA

We consider hyperfine components of rovibrational transition between the $(\nu_\mathrm{i}, N_\mathrm{i})$ and $(\nu_\mathrm{f}, N_\mathrm{f})$ states, where, ν and N are the vibrational and rotational quantum numbers, respectively. Due to hyperfine interactions, both levels are split into states which, following Refs. [19,20,22,24,25,41], we label as $|\nu_\mathrm{i}; N_\mathrm{i} F_\mathrm{i} m_{\mathrm{F_i}}(\pm)_\mathrm{i}\rangle$ and $|\nu_\mathrm{f}; N_\mathrm{f} F_\mathrm{f} m_{\mathrm{F_f}}(\pm)_\mathrm{f}\rangle$, respectively [42]. Here, F is the total angular momentum quantum number (the eigenvalue of the square of the total angular momentum, $\mathbf{F}$) which originates from the coupling of three angular momenta: the rotational angular momentum $\mathbf{N}$ and the nuclear spin angular momenta of the two nuclei, $\mathbf{I}_1$ and $\mathbf{I}_2$. m_F denotes the projection of the total angular momentum on the space-fixed axis of quantization. The meaning of the $(\pm)$ label, as well as a summary of the coupling schemes, coupled basis, and the eigenstates of the hyperfine Hamiltonian, is provided in Appendix A.

In the first step, we assume that each hyperfine component (HF) of the rovibrational transition is infinitely sharp. Such a spectrum is referred to as the stick spectrum [18]. The first distribution moment of the hyperfine spectrum is defined as a sum of products of position and intensity of each (HF-labeled) hyperfine component,

$$\mathcal{M}_\mathrm{fi}^{(1)} = \sum_\mathrm{HF} \left(\nu_\mathrm{fi}^\mathrm{HF} - \nu_\mathrm{fi}\right) \frac{S_\mathrm{fi}^{n\mathrm{HF}}}{S_\mathrm{fi}^{n}}, \tag{1}$$

where $(\nu_\mathrm{fi}^\mathrm{HF} - \nu_\mathrm{fi})$ is the position of a single HF component with respect to the central frequency of a rovibrational transition, and $S_\mathrm{fi}^{n\mathrm{HF}}/S_\mathrm{fi}^{n}$ is the ratio of the intensity of a HF component to the intensity of the HF-unresolved transition. The top index denotes the rank of the spectroscopic transition: $n = 1$ corresponds to the electric dipole transition and $n = 2$ corresponds to the electric quadrupole transition. The formulas for $S_\mathrm{fi}^{n\mathrm{HF}}$ and S_fi^{n} depend on the rank of the transition and the considered branch. We proposed a generic form of the $S_\mathrm{fi}^{n\mathrm{HF}}/S_\mathrm{fi}^{n}$ ratio in Ref. [41], which we refer to as the relative intensity of a given HF component,

$$\frac{S_\mathrm{fi}^{n\mathrm{HF}}}{S_\mathrm{fi}^{n}} = \frac{|\langle \nu_\mathrm{f}; N_\mathrm{f} F_\mathrm{f}(\pm)_\mathrm{f}||\mathrm{T}^{(n)}(\mathbf{M})||\nu_\mathrm{i}; N_\mathrm{i} F_\mathrm{i}(\pm)_\mathrm{i}\rangle|^2}{w_I f_n(N_\mathrm{i}, N_\mathrm{f})\left|\mathbf{M}_\mathrm{fi}^{n}\right|^2}. \tag{2}$$

Here, $\mathbf{M}^n$ is the multipole moment of the rovibrational transition and corresponds to the electric dipole moment $\mathbf{d}$ $(n = 1)$ and for the electric quadrupole moment $\mathcal{Q}$ for $(n = 2)$. The reader is referred to Ref. [41] for the explicit formulas for $S_\mathrm{fi}^{n\mathrm{HF}}$ and S_fi^{n} for electric dipole and quadrupole transitions. In the following part of the derivation, we use the formalism of spherical tensor algebra [43]. We introduce $T^{(n)}(\mathbf{M})$, an irreducible spherical tensor of rank n, which describes the proper multipole moment. w_I is the nuclear degeneracy factor of the initial rovibrational state, which equals $(2I_1 + 1)(2I_2 + 1)$ for the heteronuclear isotopologues and $(2I + 1)$ for the homonuclear species. The $f_n(N_\mathrm{i}, N_\mathrm{f})$ term depends on the rank of the transition and the branch considered and originates from the transformation of the multipole moment between the molecule-fixed and the space-fixed frame of reference (see Appendix A of Ref. [41]).

The position of each hyperfine component with respect to the central frequency of a rovibrational transition, $(\nu_\mathrm{fi}^\mathrm{HF} - \nu_\mathrm{fi})$, is given by a difference between the energies of the initial and final hyperfine levels. This can be represented as the difference between the eigenvalues of the effective hyperfine Hamiltonian $\mathcal{H}^\mathrm{HF}$,

$$\left(\nu_\mathrm{fi}^\mathrm{HF} - \nu_\mathrm{fi}\right) = \frac{1}{h}\left(\langle \nu_\mathrm{f}; N_\mathrm{f} F_\mathrm{f} m_{\mathrm{F_f}}(\pm)_\mathrm{f}|\mathcal{H}^\mathrm{HF}|\nu_\mathrm{f}; N_\mathrm{f} F_\mathrm{f} m_{\mathrm{F_f}}(\pm)_\mathrm{f}\rangle - \langle \nu_\mathrm{i}; N_\mathrm{i} F_\mathrm{i} m_{\mathrm{F_i}}(\pm)_\mathrm{i}|\mathcal{H}^\mathrm{HF}|\nu_\mathrm{i}; N_\mathrm{i} F_\mathrm{i} m_{\mathrm{F_i}}(\pm)_\mathrm{i}\rangle\right). \tag{3}$$

Assuming a lack of strong hyperfine couplings between different rotational levels, it can be shown (see Appendix B 1) that the first distribution moment corresponds to the difference between the sum of the diagonal elements of the effective hyperfine Hamiltonian in the two rovibrational states. For the coupling scheme suitable for homonuclear diatomics, this is given as

$$\mathcal{M}_\mathrm{fi}^{(1)} = \frac{1}{hw_I}\left\{\frac{1}{2N_\mathrm{f}+1}\sum_{I_\mathrm{f}, F_\mathrm{f}, m_{\mathrm{F_f}}} \langle \nu_\mathrm{f}; [N_\mathrm{f}(I_1 I_2)I_\mathrm{f}]F_\mathrm{f} m_{\mathrm{F_f}}|\mathcal{H}^\mathrm{HF}|\nu_\mathrm{f}; [N_\mathrm{f}(I_1 I_2)I_\mathrm{f}]F m_{\mathrm{F_f}}\rangle - \frac{1}{2N_\mathrm{i}+1}\sum_{I_\mathrm{i}, F_i, m_{\mathrm{F_i}},} \langle \nu_i; [N_i(I_1 I_2)I_\mathrm{i}]F_i m_{\mathrm{F_i}}|\mathcal{H}^\mathrm{HF}|\nu_i; [N_i(I_1 I_2)I_\mathrm{i}]F_i m_{\mathrm{F_i}}\rangle\right\}. \tag{4}$$

TABLE I. Tensorial form of the leading hyperfine interactions in the homo- and heteronuclear isotopologues of molecular hydrogen. For a discussion of the hyperfine interactions, as well as for formulas of matrix elements of the hyperfine Hamiltonian, see Refs. [19,20,22].

Hyperfine interaction	Homonuclear case	Heteronuclear case
Nuclear spin-rotation	$c_{\rm nsr} T^{(1)}(\mathbf{N}) \cdot T^{(1)}(\mathbf{I})$	$\sum_j c_{\rm nsr_j} T^{(1)}(\mathbf{N}) \cdot T^{(1)}(\mathbf{I}_j)$
Nuclear spin–nuclear spin dipole	$c_{\rm dip} T^{(2)}(\mathbf{C}) \cdot T^{(2)}(\mathbf{I}_1, \mathbf{I}_2)$	$c_{\rm dip} T^{(1)}(\mathbf{I}_2) \cdot T^{(1)}(\mathbf{C}, \mathbf{I}_1)$
Electric quadrupole	$\sum_j T^{(2)}(\nabla \mathbf{E}_j) \cdot T^{(2)}(\mathbf{Q}_j)$	$\sum_j T^{(2)}(\nabla \mathbf{E}_j) \cdot T^{(2)}(\mathbf{Q}_j)$

The corresponding formula for the coupling scheme suitable for heteronuclear species is provided in Appendix B 2. The effective hyperfine Hamiltonian can be represented as a series expansion of spherical tensor operators which represent (electric or magnetic) nuclear moments, $T^{(k)}(\mathcal{A})$, and (electric or magnetic) fields generated by the electrons and nuclei and derivatives of these fields, $T^{(k)}(\mathcal{B})$ [43–46],

$$\mathcal{H}^{\rm HF} = \sum_{k \geqslant 1} T^{(k)}(\mathcal{A}) \cdot T^{(k)}(\mathcal{B}). \tag{5}$$

Each term in this expansion is, in fact, a scalar product of spherical tensor operators, defined as

$$T^{(k)}(\mathcal{A}) \cdot T^{(k)}(\mathcal{B}) = \sum_{q=-k}^{k} T_q^{(k)}(\mathcal{A}) T_{-q}^{(k)}(\mathcal{B}), \tag{6}$$

where q denotes the $(2k+1)$ components of the spherical tensors. For the hydrogen molecule, the leading hyperfine interactions involve the nuclear spin-rotation interaction, the nuclear spin–nuclear spin dipole interaction, and, for the deuterium-bearing species, the interaction of the nuclear electric quadrupole moment with molecular electric field gradient (see Table I). We note that the notation in Eq. (5) (which stems from Ref. [43]) might be ambiguous in this context, as the hyperfine Hamiltonian can contain more than one term of rank k, i.e., in the homonuclear case, we consider two terms of rank $k = 2$, while in the heteronuclear case, we have two terms of rank $k = 1$ (see Table I).

Matrix elements of the effective hyperfine Hamiltonian in Eq. (4), which has a generic form introduced in Eq. (5), are evaluated using spherical tensor algebra. For the two irreducible spherical operators which act on two distinct components of the coupled basis, matrix elements are given as [47]

$$\begin{aligned}
&\langle \nu; (j_1 j_2) j m | T^{(k)}(\mathcal{A}) \cdot T^{(k)}(\mathcal{B}) | \nu; (j_1 j_2) j m \rangle \\
&\quad = (-1)^{j_1 + j + j_2} \begin{Bmatrix} j_2 & j_1 & j \\ j_1 & j_2 & k \end{Bmatrix} \\
&\qquad \times \langle n u; j_1 || T^{(k)}(\mathcal{A}) || \nu; j_1 \rangle \langle \nu; j_2 || T^{(k)}(\mathcal{B}) || \nu; j_2 \rangle.
\end{aligned} \tag{7}$$

Putting $j_1 = N$, $j_2 = I$, $j = F$, and $m = m_{\rm F}$ and summing over I, F, and $m_{\rm F}$ leads to (see Appendix C)

$$\begin{aligned}
&\sum_{I,F,m_{\rm F}} \langle \nu; (NI) F m_{\rm F} | T^{(k)}(\mathcal{A}) \cdot T^{(k)}(\mathcal{B}) | \nu; (NI) F m_{\rm F} \rangle \\
&\quad = \delta_{k0} [\sqrt{(2N+1)} \langle \nu; N || T^{(k)}(\mathcal{A}) || \nu; N \rangle] \\
&\qquad \times \left[\sum_I \sqrt{(2I+1)} \langle I || T^{(k)}(\mathcal{B}) || I \rangle \right],
\end{aligned} \tag{8}$$

which means that the sum vanishes unless $k = 0$. As mentioned earlier, each hyperfine interaction is represented by a scalar product of two spherical tensors of rank at least 1. This means that both sums in Eq. (4) vanish and, as a consequence, the first distribution moment of the hyperfine stick spectrum is zero,

$$\mathcal{M}_{\rm fi}^{(1)} = 0. \tag{9}$$

A similar derivation can be performed for the heteronuclear isotopologues, although some of the tensorial forms recalled in Table I do not fulfill the condition (7) immediately. Indeed, the nuclear spin rotation associated with the I_2 nuclear spin, as well as the dipole interaction, involve the product of two spherical tensors which act either on the subspace of the $\mathbf{I}_2$ or the coupled subspace of the $\mathbf{F}_1$ angular momentum. The detailed analysis is presented in Appendix B 2.

We have numerically confirmed Eq. (9) for all 86 105 electric dipole and electric quadrupole transitions in the six isotopologues of hydrogen, which were studied in Refs. [19,20,20,22,24]. The result derived here is based on an assumption that the hyperfine-induced coupling between different rotational levels is negligible in comparison to the energy difference between rotational states. This condition is fulfilled by diatomic molecules in the $^1\Sigma$ state and, in particular, by molecular hydrogen. The isotopologues of hydrogen possess large rotational constants ($B = 60.853$ cm^{-1} for H_2 [48]) and are characterized by hyperfine interactions that are several orders of magnitude smaller than the rotational energy intervals. The result derived here should be of interest to the accurate spectroscopy of the light hydrogen halides, such as HF and HCl, or isotopologues of carbon monoxide that possess hyperfine structure (^{13}C ^{16}O or ^{12}C ^{17}O). For heavier $^1\Sigma$ diatomics, the ratio of the largest hyperfine coupling constant to the rotational constant grows considerably, and the inclusion of the N and $N' = N \pm 2$ couplings is necessary for an accurate description of the molecular spectra [see the discussion after Eq. (A3) in Appendix A].

III. DOPPLER-BROADENED SPECTRA

The shape of the spectrum is a result of various physical processes that perturb molecular transitions. Thermal motion of molecules gives rise to the Doppler broadening, while collisions lead to the pressure broadening and shift of the spectral lines [49]. Shapes of optical resonances in molecular hydrogen deviate considerably from the commonly used Voigt profile [50,51]. An accurate description of beyond-Voigt lineshape effects is crucial for determining the central frequency of the observed transition [14].

Here, we analyze the spectra in the low-pressure regime, where collisional broadening and shift of spectral lines are

negligible, and the primary broadening mechanism stems from the Doppler effect. In such a case, the shape of an isolated line is described by the Gaussian function. Here, we acknowledge the presence of the underlying hyperfine structure of the resonance and we consider the spectrum which involves the sum of N Gaussian functions, which are centered at frequencies of respective hyperfine components. However, unless the experimental spectra are collected at temperatures low enough to distinguish between single components, the hyperfine components are blended into a single line.

The position of the maximum of such spectrum can be determined as follows. First, one can fit the experimental data with the sum of N Gaussian functions. The number of hyperfine components can be large and, as they are spread on a relatively small range of frequencies, numerical problems might lead to incorrect determination of the maximum. Second, one might calculate the first moment of the measured spectra $[f_{\rm exp}(\nu)]$ numerically,

$$\mathcal{M}_{\rm fi}^{(1)} = \int_{\nu_{\rm min}}^{\nu_{\rm max}} d\nu \nu f_{\rm exp}(\nu), \tag{10}$$

where $\nu_{\rm min}$ and $\nu_{\rm max}$ denote the range of the experimental frequency scan. However, as this procedure involves numerical integration over a wide range of frequencies, large experimental noise, which is present at frequencies far from $\nu_{\rm fi}$, might lead to an incorrect determination of the resulting central frequency. Ultimately, in certain cases, one can determine the central frequency as the numerical derivative of the measured spectra and look for ν, for which the derivative vanishes (see Appendix D). This corresponds to the position of the maximum of the measured spectra. We discuss this approach at the end of the following section.

A. Analytical considerations

We consider the spectrum which involves N Gaussian functions of the form

$$f^{\rm HF}(\nu) = \frac{A^{\rm HF}}{\sqrt{\pi}\nu_D} e^{-(\nu-\nu_{\rm fi}^{\rm HF})^2/\nu_D^2}, \tag{11}$$

where $\nu_D = \frac{\nu_{\rm fi}^{\rm HF}}{c}\sqrt{2k_BT/m}$ is related to the half width at half maximum (HWHM) of the Doppler profile, $\Gamma_D = \sqrt{\ln 2}\nu_D$, and $A^{\rm HF} = S_{\rm fi}^{\rm HF}/S_{\rm fi}$ is the relative (unitless) intensity of each hyperfine component, defined in Eq. (2). Since hyperfine components are distributed in close vicinity (of the order of 10^6 Hz or less) of the central frequency of the rovibrational transition (which is of the order of 10^{12}–10^{15} Hz), we can approximate $\nu_{\rm fi}^{\rm HF} \approx \nu_{\rm fi}$ and we can assume that each hyperfine component has the same Doppler width. The latter assumption is well justified since the Doppler width of rovibrational lines in molecular hydrogen with frequencies ranging from 10^{12} (for pure rotational transitions) to 10^{15} Hz (for the highest overtones) is modified by less than 10^{-6} on a narrow range of frequencies of the order of 10^6 Hz. In such a case, the first distribution moment of the total spectrum is given by

$$\mathcal{M}_{\rm fi}^{(1)} = \int_{-\infty}^{\infty} d\nu \nu \sum_{\rm HF} f^{\rm HF}(\nu) = \sum_{\rm HF} A^{\rm HF}\nu_{\rm fi}^{\rm HF}, \tag{12}$$

where the symbol HF denotes the sum of all hyperfine components of the spectrum. Here, we used the fact that the first moment of a Gaussian distribution centered at $\nu_{\rm fi}$ is simply $\nu_{\rm fi}$. As shown in the previous section, the result is exactly zero for *all* rovibrational transitions in the hydrogen molecule. This means that when the spectrum is measured in the low-pressure regime, where the shape of the spectral transition is determined by a Gaussian function, the presence of the hyperfine structure does not affect the central frequency of the Doppler-limited rovibrational transition.

We briefly discuss finding the maximum of the spectrum through the derivative of the spectrum. One has to realize the obvious limitation of this approach: if the hyperfine components can at least be partially resolved, roots of the numerical derivative will point to the various local maxima and minima of the spectrum, and not to the barycenter of the transition. Careful analysis of the derivative of the spectrum consisting of N Gaussians might indicate the range of validity of the results presented in this work.

In Appendix D, we prove that the maximum of the spectrum consisting of N Gaussians of the same width ν_D, which are spread over the narrow range of frequencies (significantly smaller than ν_D), is

$$\nu^{\rm max\,(N)} \approx \sum_{i=1}^{N} \nu_{0i}\bar{C}_i, \tag{13}$$

where $\nu_{0\,i}$ and $\bar{C}_i = C_i/(\sum_j C_j)$ denote the center and the relative height of the ith Gaussian, respectively. This corresponds to the barycenter of the resulting spectrum, which, for the case of rovibrational transitions with hyperfine structure, is 0 [Eq. (9)].

B. Numerical confirmation—four rovibrational transitions in molecular hydrogen

We numerically test the range of validity of the obtained results on four rovibrational transitions in the three isotopologues of hydrogen. First, similar to Ref. [52], we define a dimensionless overlapping parameter of the hyperfine components as the ratio between the HWHM of the line profile (here Γ_D) and the mean-square hyperfine splitting,

$$\Omega = \frac{\Gamma_D}{\sqrt{\sum_i \left(A_i^{\rm HF}\nu_i^{\rm HF}\right)^2}}. \tag{14}$$

We note that the root-mean-square hyperfine splitting is of the order of 10^1 kHz for most of the rovibrational transitions in H_2, HD, and D_2. In the next step, we simulate four chosen rovibrational transitions as a sum of Gaussian functions $[\sum_{\rm HF} f^{\rm HF}(\nu)$, with $f^{\rm HF}(\nu)$ defined in Eq. (11)] and we look for the maximum of the spectrum, $\nu^{\rm max}$. When the hyperfine components are well resolved, $\nu^{\rm max}$ corresponds to the position of the hyperfine component with the largest intensity. We analyze the 2-0 R(1) line in HD, studied by Doppler-limited spectroscopy in Refs. [15,32,40], the 1-0 R(0) line in HD, which has the lowest absolute uncertainty of all rovibrational transitions in molecular hydrogen [11], the 2-0 S(2) line in D_2, analyzed by cavity-enhanced techniques in Refs. [14,28,29,35], and the 1-0 Q(1) line in H_2, investigated

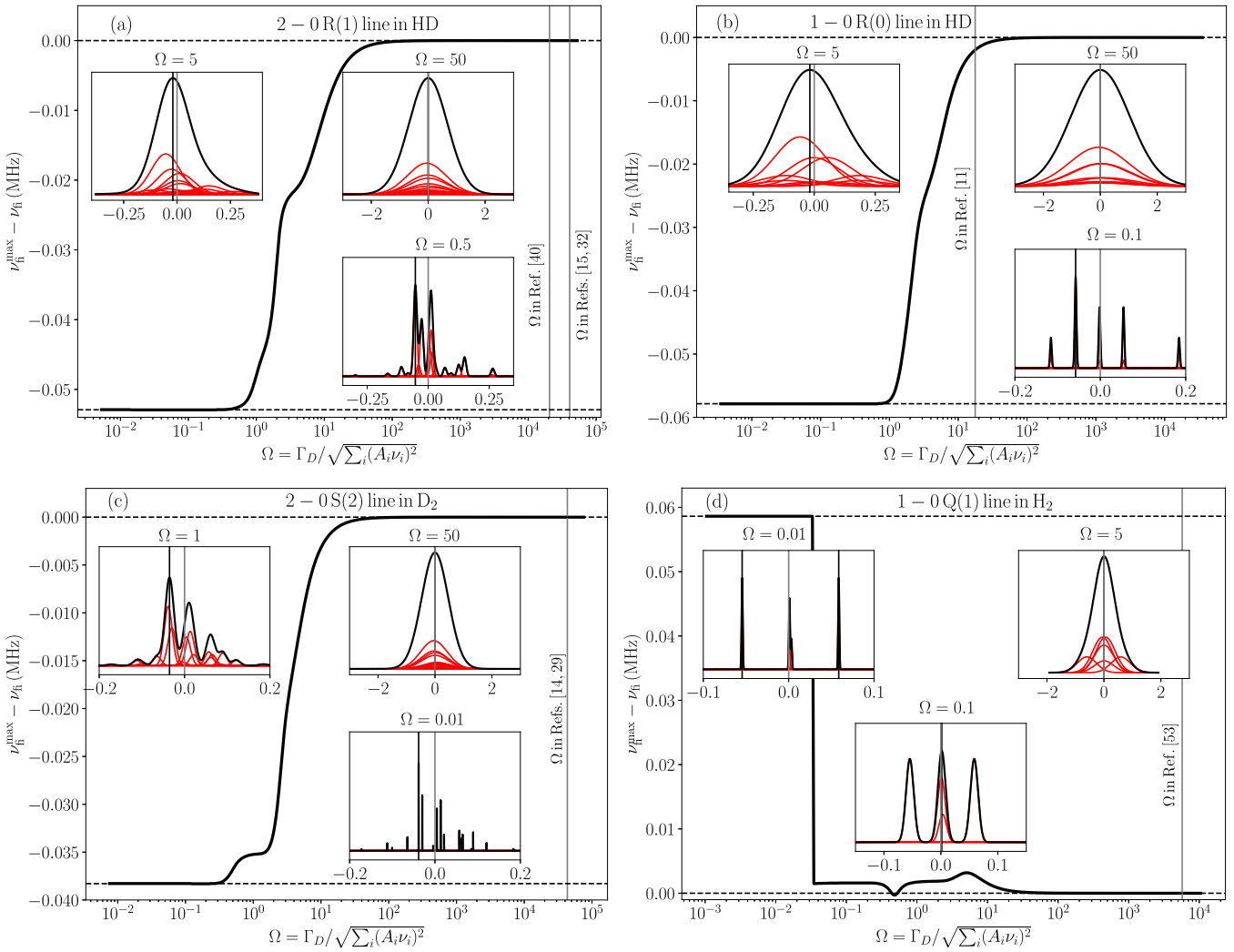

FIG. 1. Position of the maximum of rovibrational spectra, $\nu_{\rm fi}^{\rm max}$, with respect to the HFS-free transition frequency $\nu_{\rm fi}$, as a function of the dimensionless hyperfine overlapping parameter Ω [defined in Eq. (14)], for the four chosen transitions in molecular hydrogen. The gray vertical lines correspond to values of Ω in selected recent experiments (see the main text for details). The black vertical dashed lines in each panel correspond to the low- and high-Ω limits of $\nu_{\rm max}$, i.e., the position of the strongest hyperfine component and the HFS-free transition frequency, respectively. The inset figures present the Doppler-broadened spectra for the fixed Ω—the red curves correspond to individual hyperfine components, while the black curve is the total spectrum, resulting from summing individual components. We put two vertical lines in each inset plot—the gray line corresponds to the HFS-free frequency and the black line denotes $\nu_{\rm fi}^{\rm max}$.

recently using stimulated Raman spectroscopy [53]. The results are presented in Fig. 1.

Both transitions in HD exhibit a typical $\nu_{\rm fi}^{\rm max}(\Omega)$ dependence: at low values of Ω (well-resolved hyperfine components), the maximum of the spectrum simply corresponds to the position of the hyperfine component with the largest intensity [$\nu_{\rm fi}^{\rm max} = -52.9$ kHz and -57.8 kHz for the 2-0 R(1) and 1-0 R(0) line, respectively]. As Ω increases, the components blend into one line and the position of the maximum shifts towards the HFS-free frequency, which is achieved for $\Omega \approx 50$. The gray vertical lines in each panel correspond to the value of Ω in respective experiments. For the 2-0 R(1) line, Doppler HWHM at room temperature is 775 MHz, which [since $\sqrt{\sum_i (A_i^{\rm HF}\nu_i^{\rm HF})^2} \approx 19$ kHz for this line] gives $\Omega \approx 4\times10^4$. Thus, the underlying 21 hyperfine components have no visible effect on the position of the maximum of the 2-0 R(1) line, not only at room temperature [15,32] but also at 80 K, as reported by Kassi *et al.* [40] ($\Omega \approx 2\times10^4$ at 80 K). We note here that collisional effects had a significant impact on the measurements performed by the Caserta group, and thus the Gaussian model analyzed here may not be directly applicable to the interpretation of the spectra studied in Refs. [15,32].

The experiment of Fast and Meek was performed in a different, low-density regime, using a supersonic molecular beam [11] that offers much lower effective transverse temperature, resulting in a sub-MHz Doppler broadening. The gray vertical line in the top right panel of Fig. 1 corresponds to $\Omega \approx 18$ since the mean-square hyperfine splitting is approximately 30 kHz for the 1-0 R(0) line and the authors of Ref. [11] assumed that the underlying Gaussians have equal HWHMs of 400–500 kHz. We note here that the analysis of

the hyperfine structure in Ref. [11] was more complex than the one presented here, due to the double-resonance nature of the experimental technique—a subsequent two-photon UV excitation from the $\nu = 1, N = 1$ state influenced the relative intensities of the hyperfine components of the 1-0 R(0) transition.

A slightly different dependence of $\nu_{\text{fi}}^{\max}$ on (Ω) is seen for the 2-0 S(2) line in D_2. For $\Omega \sim 10^{-2}$, $\nu_{\text{fi}}^{\max}$ corresponds to the position of the largest hyperfine component ($\nu_{\text{fi}}^{\max} = -38.3$ kHz). As Ω increases, $\nu_{\text{fi}}^{\max}$ shifts towards -35 kHz (the plateau near $\Omega = 1$), due to the vicinity of the second most intense hyperfine component at -29.7 kHz. Then, as Ω becomes larger than 1, the 22 components blend into a single line. The gray vertical line denotes $\Omega \approx 4.3\times10^4$ in Refs. [14,29] [$\Gamma_D \approx 570$ GHz and $\sqrt{\sum_i (A_i^{\text{HF}}\nu_i^{\text{HF}})^2} \approx 13$ kHz].

Finally, we present an atypical example of $\nu_{\text{fi}}^{\max}(\Omega)$ dependence—the case of the 1-0 Q(1) line in H_2, recently studied by Lamperti *et al.* [53]. This transition involves six hyperfine components which are spread almost symmetrically with respect to the HFS-free frequency (the remaining two components at -600 kHz and 587 kHz are not visible on the inset plots in the bottom right panel of Fig. 1). The two components located at -54 and 59 kHz have the same relative intensity (on the bottom right panel of Fig. 1, we associate $\nu_{\text{fi}}^{\max}$ with the 59 kHz component). As Ω increases, the two, less intense peaks located in the vicinity of the HFS-free frequency blend into one line, which is more intense than the other components—this corresponds to the sudden drop of $\nu_{\text{fi}}^{\max}(\Omega)$ for $\Omega \approx 3\times10^{-2}$. For larger values of Ω, $\nu_{\text{fi}}^{\max}$ remains within the 3 kHz distance from the central frequency and tends to HFS free for $\Omega > 10$. This is the case for the study of Lamperti *et al.* [53], where $\Omega \approx 5.7\times10^3$ justifies neglecting the hyperfine structure in the experimental analysis.

The four spectroscopic transitions considered here confirm that if the hyperfine components are spread over a narrow range of frequencies compared to the Doppler width, there is no significant shift of the resulting spectrum. Using the overlapping parameter Ω to quantify the ratio of ν_D to the mean-square hyperfine splitting indicates that no visible hyperfine shift is present if $\Omega > 50$. For instance, for the case of the 1-0 R(0) line in HD, $\Omega = 50$ corresponds to the temperature of approximately 4 mK. In some cases, such as the Q lines in H_2, this condition is obeyed for even smaller values of Ω.

IV. CONCLUSION

We analyzed the first distribution moment of the hyperfine stick spectra. Based on a well-justified assumption about the form of the hyperfine Hamiltonian and the negligible mixing between rotational states, we showed that the barycenter is related to a difference between the sum of diagonal elements of the hyperfine Hamiltonian in the initial and final spectroscopic states, respectively. Additionally, we showed that the sum of diagonal elements of a scalar product of two spherical tensors vanishes unless the two tensors are of rank 0. This allowed us to state that the first distribution moment of the hyperfine spectra vanishes.

In the next step, we analyzed the barycenter of the Doppler-broadened spectra. We assumed that each hyperfine component is described by the Gaussian function of the same width and we have shown that the formula depends on exactly the same factor as in the case of the hyperfine stick spectrum. We also calculated the maximum of the resulting spectra (by searching for roots of the derivative of the total spectrum) for the case in which the Doppler width is significantly larger than the underlying hyperfine structure. The resulting formula involved the first distribution moment of the stick spectrum, and thus vanishes.

Finally, we tested the extent to which the results derived here are applicable to the four selected rovibrational transitions in the three isotopologues of hydrogen. By introducing a dimensionless overlapping parameter Ω (the ratio of Γ_D to the mean-square hyperfine splitting), we confirmed that there is no net hyperfine shift for $\Omega > 50$. This allowed us to conclude that in the accurate experimental spectra performed in the low-pressure regime, there should be no significant shift due to the underlying, unresolved hyperfine spectra. This result should be of particular importance for the recent Doppler-limited studies of the rovibrational structure of hydrogen [14,15,32]. We note that the formulas derived here should be valid for any diatomic molecule for which the hyperfine-induced mixing is negligible. Molecular hydrogen, with its exceptionally large rotational constant, fulfills this condition particularly well.

The work presented here is a stepping stone toward a deeper understanding of the influence of hyperfine structure on accurate molecular spectra, which are used to study quantum electrodynamics and put constraints on physics beyond the standard model. However, the majority of Doppler-limited studies suffer from collisional effects, which are not considered here. A natural extension of this work would be to study the existence of a net hyperfine shift in collision-perturbed spectra. For instance, a limiting case, opposite to the one presented here, could be considered: at high pressure and low temperature, the total spectrum should be a sum of Lorentzian functions corresponding to individual hyperfine components. We can immediately state that the results obtained here are not applicable to the Lorentzian case. We recall that one of the assumptions used here is that the hyperfine components have the same width. This is not fulfilled in the collision-perturbed case since the individual hyperfine components of molecular transitions are known to have different pressure broadening and shift coefficients. For instance, Buffa *et al.* [54] reported a significant variability ($\approx$30%) of the pressure-broadening coefficients in the hyperfine structure of the rotational transition in CH_3I. Interestingly, the hyperfine collisional effects are expected to be less pronounced in linear molecules, as explained by Belli *et al.* [55], and confirmed numerically by Green for He-perturbed rotational lines in HCN [56] and by Buffa and Tarini for He-perturbed DCO^+ lines [52,57]. Collisional effects in the hyperfine structure of molecular hydrogen seem to be particularly interesting: hydrogen lines are known to have an exceptionally large pressure shift [50], which can exceed pressure broadening [58]. If a significant variability in the pressure-shift coefficients is found for individual hyperfine components, the order of the particular components could be different than in the Doppler-broadened case. Moreover, line coupling between different hyperfine components, which has been detected in the rotational spectrum of HI [59], could lead

to a severe deterioration of the total shape of the spectrum, at least in the intermediate range of Ω (for pressures large enough to induce overlapping of the components, but not large enough to blend them into a single line). The study of collisional effects in the hyperfine structure of molecular hydrogen will be the subject of upcoming papers.

ACKNOWLEDGMENTS

The research is financed from the budgetary funds on science projected for 2019–2023 as a research project under the "Diamentowy Grant" program. P.W. is supported by the National Science Centre in Poland, Project No. 2019/35/B/ST2/01118. The research is a part of the program of the National Laboratory FAMO in Toruń, Poland. Calculations have been partially carried out using resources provided by the Wroclaw Centre for Networking and Supercomputing [60], Grant No. 546. We gratefully acknowledge Polands high-performance computing infrastructure PLGrid (HPC Centers: ACK Cyfronet AGH, PCSS, CI TASK) for providing computer facilities and support within computational Grant No. PLG/2022/015576.

APPENDIX A: COUPLING SCHEMES AND HYPERFINE EIGENSTATES

The effective hyperfine Hamiltonian for a given electronic state in the six isotopologues was discussed in Refs. [19,20,22,24,25]. Here, we discuss only the parts relevant for this paper, namely, the coupled basis used in the derivation, and the relation between the coupled basis and the eigenbasis of the hyperfine Hamiltonian.

Throughout the paper, we use the eigenbasis of the square of the total angular momentum, $\mathbf{F}$, which is constructed by coupling eigenvectors of the three angular momenta: $\mathbf{I}_1$, $\mathbf{I}_2$, and $\mathbf{N}$. For the homonuclear isotopologues of hydrogen, we couple the two nuclear spin angular momenta to form the total nuclear spin angular momentum $\mathbf{I}$, which is coupled to the rotational angular momentum $\mathbf{N}$ to form the total angular momentum $\mathbf{F}$. The resulting state vector is denoted as $|\nu;[N(I_1I_2)I]Fm_\mathrm{F}\rangle$ and is given by

$$\begin{aligned}|\nu;[N(I_1I_2)I]Fm_\mathrm{F}\rangle &= \sum_{m_\mathrm{N}=-N}^{N}\sum_{m_\mathrm{I}=-I}^{I}\langle Nm_\mathrm{N}Im_\mathrm{I}|Fm_\mathrm{F}\rangle|\nu;Nm_\mathrm{N}\rangle|(I_1I_2)Im_\mathrm{I}\rangle \\ &= \sum_{m_\mathrm{N}=-N}^{N}\sum_{m_\mathrm{I}=-I}^{I}\langle Nm_\mathrm{N}Im_\mathrm{I}|Fm_\mathrm{F}\rangle\sum_{m_{\mathrm{I}_1}=-I_1}^{I_1}\sum_{m_{\mathrm{I}_2}=-I_2}^{I_2}\left\langle I_1m_{\mathrm{I}_1}I_2m_{\mathrm{I}_2}\middle|Im_\mathrm{I}\right\rangle\left|\nu;Nm_\mathrm{N}\right\rangle\left|I_1m_{\mathrm{I}_1}\right\rangle\left|I_2m_{\mathrm{I}_2}\right\rangle, \end{aligned} \tag{A1}$$

where $\langle\cdot|\cdot\rangle$ is the Clebsch-Gordan coefficient, $|I_1m_{\mathrm{I}_1}\rangle$ and $|I_2m_{\mathrm{I}_2}\rangle$ are the eigenvectors of $\mathbf{I}_1^2$ and $\mathbf{I}_2^2$, respectively, and $|\nu;Nm_\mathrm{N}\rangle = |\nu N\rangle|Nm_\mathrm{N}\rangle$ denotes the rovibrational level. In position representation, $|\nu;Nm_\mathrm{N}\rangle$ is given as

$$\langle\vec{\mathbf{R}}|\nu;Nm_\mathrm{N}\rangle = \chi_{\nu,N}(R)Y_{Nm_N}(\hat{\mathbf{R}}). \tag{A2}$$

$\vec{\mathbf{R}}$ denotes the position vector of the internuclear axis, $\chi_{\nu,N}(R)$ is the solution of the nuclear radial Schrödinger equation, and Y_{Nm_N} is the spherical harmonic.

In the heteronuclear case, one of the nuclear spin angular momenta, $\mathbf{I}_1$, is coupled to the rotational angular momentum to form the intermediate angular momentum $\mathbf{F}_1$. The latter is coupled to the remaining nuclear spin angular momentum $\mathbf{I}_2$ to form the total angular momentum $\mathbf{F}$. The resulting vector is denoted as $|\nu;[(NI_1)F_1I_2]Fm_\mathrm{F}\rangle$,

$$\begin{aligned}|\nu;[(NI_1)F_1I_2]Fm_\mathrm{F}\rangle &= \sum_{m_{\mathrm{F}_1}=-F_1}^{F_1}\sum_{m_{\mathrm{I}_2}=-I_2}^{I_2}\langle F_1m_{\mathrm{F}_1}I_2m_{\mathrm{I}_2}|Fm_\mathrm{F}\rangle\left|\nu;(NI_1)F_1m_{\mathrm{F}_1}\right\rangle\left|I_2m_{\mathrm{I}_2}\right\rangle \\ &= \sum_{\mathrm{m}_{\mathrm{F}_1}=-\mathrm{F}_1}^{F_1}\sum_{\mathrm{m}_{\mathrm{I}_2}=-\mathrm{I}_2}^{I_2}\left\langle F_1m_{\mathrm{F}_1}I_2m_{\mathrm{I}_2}\middle|Fm_\mathrm{F}\right\rangle\sum_{m_\mathrm{N}=-N}^{N}\sum_{m_{\mathrm{I}_1}=-I_1}^{I_1}\left\langle Nm_\mathrm{N}I_1m_{\mathrm{I}_1}\middle|F_1m_{\mathrm{F}_1}\right\rangle\left|\nu;N\right\rangle\left|I_1m_{\mathrm{I}_1}\right\rangle\left|I_2m_{\mathrm{I}_2}\right\rangle. \end{aligned} \tag{A3}$$

The effective hyperfine Hamiltonian is diagonal with respect to F and m_F. In the case of homonuclear molecules, the nuclear spin–nuclear spin dipole and, in the case of D_2, the quadrupole interaction introduce a weak coupling between the N and $N' = N \pm 2$ states. This coupling is, however, at least seven orders of magnitude smaller than the energy interval between the N and $N' = N \pm 2$ states, and is therefore neglected in the analysis. The relative weakness of this coupling with respect to the rotational constant is particularly pronounced in hydrogen isotopologues, but it should also hold for light hydrogen halides, such as HF and HCl, as well as for the less abundant isotopologues of carbon monoxide. The ratio of the largest hyperfine coupling constant in the $\nu = 0, N = 1$ state to the rotational constant, hereafter referred to as γ, is of the order of 10^{-7} for $\mathrm{H}\,^{19}\mathrm{F}$ [61], 10^{-5} for $^{12}\mathrm{C}\,^{17}\mathrm{O}$ and $^{13}\mathrm{C}\,^{17}\mathrm{O}$ [62,63], and 10^{-4} for $\mathrm{H}\,^{35}\mathrm{Cl}$ and $\mathrm{H}\,^{37}\mathrm{Cl}$ [64]. Indeed, in the analysis of hyperfine-resolved rotational spectra [62,64] or molecular-beam electric resonance spectra [61,65] of these species, the couplings between the N and $N' = N \pm 2$ levels were neglected. Moving down the periodic table, we note that $\gamma \sim 10^{-3}$ for $\mathrm{H}\,^{79}\mathrm{Br}$ and $\mathrm{H}\,^{81}\mathrm{Br}$ [66], and $\gamma \sim 10^{-2}$ for the $\mathrm{H}\,^{127}\mathrm{I}$ [67,68]. In these cases, couplings between different rotational levels are crucial for accurate analysis of the hyperfine spectra [66,67]. While in the case of Doppler-limited spectroscopy large γ is undesirable, strong hyperfine

coupling might enhance the hypothetical Feshbach resonances in collisions of two $^1\Sigma$ molecules, as predicted by Wallis and Krems for ^{87}Rb ^{133}Cs ($\gamma \sim 10^{-3}$) [69].

In the homonuclear case, the nuclear spin–nuclear spin and the electric quadrupole interaction also couple the I and $I' = I \pm 2$ states. In the case of hydrogen molecules, considered here, this coupling is only of relevance for *ortho*-D_2. In this case, to obtain the hyperfine eigenstates, the F-labeled blocks should be diagonalized. The relation between the hyperfine eigenstates and the coupled basis vectors is

$$|\nu; NFm_F(\pm)\rangle = \sum_I a_I^{\nu NF(\pm)} |\nu; [N(I_1I_2)I]Fm_F\rangle. \tag{A4}$$

Here, $a_I^{\nu NF(\pm)}$ is a mixing coefficient obtained from diagonalization, which is related to the hyperfine coupling constants. For *ortho*-H_2, *para*-D_2, and *ortho* $-$ T_2 ($I = 1$), the sum is trivial and the coupled basis vectors are the eigenstates of the effective hyperfine Hamiltonian. Note that this leads to an interesting consequence, as the relative intensities of rovibrational transitions in these isotopologues are independent of ν [41]. In the case of *ortho*-D_2, two out of six hyperfine states for a given rovibrational level are a superposition of the coupled basis vectors introduced in Eq. (A1). In order to distinguish these states, we use ($\pm$) labels, which denote states with higher (+) and lower ($-$) energy.

For heteronuclear isotopologues, the nuclear spin-rotation interaction associated with nuclear spin $\mathbf{I}_1$ (which was directly coupled with $\mathbf{N}$) is fully diagonal with respect to all quantum numbers. Coupling between different F_1 states occurs due to the nuclear spin rotation associated with the $\mathbf{I}_2$ spin, the nuclear spin–nuclear spin dipole interaction, and, in deuterated species, the quadrupole interaction. This imposes the necessity to diagonalize the F-labeled blocks. The hyperfine eigenstates are related to the coupled basis vectors as

$$|\nu; NFm_F(\pm)\rangle = \sum_{F_1=|F-I_2|}^{F+I_2} a_{F_1}^{\nu NF(\pm)} |\nu; [(NI_1)F_1I_2]Fm_F\rangle, \tag{A5}$$

where $a_{F_1}^{\nu NF(\pm)}$ is the mixing coefficient appropriate for the heteronuclear case. Similarly to the homonuclear case, we use the ($\pm$) labels to distinguish between the superposition states which correspond to the same values of ν, N, and F, but differ in energy.

APPENDIX B: DERIVATION OF EQ. (4)

We begin with the analysis of the first distribution moment of the following form:

$$\mathcal{M}_{\mathrm{fi}}^{(1)} = \frac{1}{h} \sum_{\mathrm{HF}} \left(\langle \nu_\mathrm{f}; N_\mathrm{f}F_\mathrm{f}m_{F_\mathrm{f}}(\pm)_\mathrm{f} | \mathcal{H}^{\mathrm{HF}} | \nu_\mathrm{f}; N_\mathrm{f}F_\mathrm{f}m_{F_\mathrm{f}}(\pm)_\mathrm{f} \rangle - \langle \nu_\mathrm{i}; N_\mathrm{i}F_\mathrm{i}m_{F_\mathrm{i}}(\pm)_\mathrm{i} | \mathcal{H}^{\mathrm{HF}} | \nu_\mathrm{i}; N_\mathrm{i}F_\mathrm{i}m_{F_\mathrm{i}}(\pm)_\mathrm{i} \rangle \right) \frac{S_{\mathrm{fi}}^{n\mathrm{HF}}}{S_{\mathrm{fi}}^{n}}. \tag{B1}$$

We consider the two terms separately. The first one is rewritten as [Eq. (2)]

$$\begin{aligned} &\sum_{\mathrm{F_i},(\pm)_\mathrm{i}} \sum_{F_\mathrm{f},(\pm)_\mathrm{f}} \langle \nu_\mathrm{f}; N_\mathrm{f}F_\mathrm{f}m_{F_\mathrm{f}}(\pm)_\mathrm{f} | \mathcal{H}^{\mathrm{HF}} | \nu_\mathrm{f}; N_\mathrm{f}F_\mathrm{f}m_{F_\mathrm{f}}(\pm)_\mathrm{f} \rangle \frac{S_{\mathrm{fi}}^{\mathrm{HF}}}{S_{\mathrm{fi}}} \\ &= \frac{1}{w_I f_n(N_\mathrm{i}, N_\mathrm{f}) |\mathbf{M}_{\mathrm{fi}}^n|^2} \sum_{\mathrm{F_i},(\pm)_\mathrm{i}} \sum_{F_\mathrm{f},(\pm)_\mathrm{f}} \langle \nu_\mathrm{f}; N_\mathrm{f}F_\mathrm{f}m_{F_\mathrm{f}}(\pm)_\mathrm{f} | \mathcal{H}^{\mathrm{HF}} | \nu_\mathrm{f}; N_\mathrm{f}F_\mathrm{f}m_{F_\mathrm{f}}(\pm)_\mathrm{f} \rangle | \langle \nu_\mathrm{f}; N_\mathrm{f}F_\mathrm{f}(\pm)_\mathrm{f} || T^{(n)}(\mathbf{M}) || \nu_\mathrm{i}; N_\mathrm{i}F_\mathrm{i}(\pm)_\mathrm{i} \rangle |^2. \end{aligned} \tag{B2}$$

We express all the terms in Eq. (B2) in the coupled basis set introduced in Eqs. (A1) and (A3) in the next two paragraphs, respectively.

1. Homonuclear case

We focus on the reduced matrix element of the transition operator. We explicitly write the modulus square of the reduced matrix element of the transition operator in the coupled basis using Eq. (A4),

$$\begin{aligned} &\sum_{\mathrm{F_i},(\pm)_\mathrm{i}} \sum_{F_\mathrm{f},(\pm)_\mathrm{f}} \langle \nu_\mathrm{f}; N_\mathrm{f}F_\mathrm{f}m_{F_\mathrm{f}}(\pm)_\mathrm{f} | \mathcal{H}^{\mathrm{HF}} | \nu_\mathrm{f}; N_\mathrm{f}F_\mathrm{f}m_{F_\mathrm{f}}(\pm)_\mathrm{f} \rangle \frac{S_{\mathrm{fi}}^{\mathrm{HF}}}{S_{\mathrm{fi}}} \\ &= \frac{1}{w_I f_n(N_\mathrm{i}, N_\mathrm{f}) |\mathbf{M}_{\mathrm{fi}}^n|^2} \sum_{\mathrm{F_i},(\pm)_\mathrm{i}} \sum_{F_\mathrm{f},(\pm)_\mathrm{f}} \langle \nu_\mathrm{f}; N_\mathrm{f}F_\mathrm{f}m_{F_\mathrm{f}}(\pm)_\mathrm{f} | \mathcal{H}^{\mathrm{HF}} | \nu_\mathrm{f}; N_\mathrm{f}F_\mathrm{f}m_{F_\mathrm{f}}(\pm)_\mathrm{f} \rangle \\ &\times \sum_{I'=|F_\mathrm{f}-N_\mathrm{f}|}^{F_\mathrm{f}+N_\mathrm{f}} a_{I'}^{(\pm)_\mathrm{f}\,*} \sum_{I''=|F_\mathrm{i}-N_\mathrm{i}|}^{F_\mathrm{i}+N_\mathrm{i}} a_{I''}^{(\pm)_\mathrm{i}} \langle \nu_\mathrm{f}; [N_\mathrm{f}(I_1I_2)I']F_\mathrm{f} || T^{(n)}(\mathbf{M}) || \nu_\mathrm{i}; [N_\mathrm{i}(I_1I_2)I'']F_\mathrm{i} \rangle \sum_{I'''=|F_\mathrm{f}-N_\mathrm{f}|}^{F_\mathrm{f}+N_\mathrm{f}} a_{I'''}^{(\pm)_\mathrm{f}} \sum_{I''''=|F_\mathrm{i}-N_\mathrm{i}|}^{F_\mathrm{i}+N_\mathrm{i}} a_{I''''}^{(\pm)_\mathrm{i}\,*} \\ &\times \langle \nu_\mathrm{f}; [N_\mathrm{f}(I_1I_2)I''']F_\mathrm{f} || T^{(n)}(\mathbf{M}) || \nu_\mathrm{i}; [N_\mathrm{i}(I_1I_2)I'''']F_\mathrm{i} \rangle^*. \end{aligned} \tag{B3}$$

The sum over $(\pm)_\mathrm{i}$ involves only the two mixing coefficients. We note that the following orthogonality relations hold:

$$\sum_{\pm} a_{I'}^{(\pm)*} a_{I''}^{(\pm)} = \delta_{I'I''}, \tag{B4}$$

$$\sum_{I} a_{I}^{(\pm)*} a_{I}^{(\pm)} = \delta_{+-}. \tag{B5}$$

In the present case, the sum over $(\pm)_\mathrm{i}$ results in the Kronecker delta $\delta_{I''I'''}$, which makes the last sum in Eq. (B3) trivial. In the next step, we simplify the two reduced matrix elements using the following property of spherical tensor operators [47]:

$$\begin{aligned}&\langle \nu_\mathrm{f}; [N_\mathrm{f}(I_1 I_2) I_\mathrm{f}] F_\mathrm{f} || T^{(n)}(\mathbf{M}) || \nu_\mathrm{i}; [N_\mathrm{i}(I_1 I_2) I_\mathrm{i}] F_\mathrm{i} \rangle \\ &\quad = \delta_{I_\mathrm{f} I_\mathrm{i}} (-1)^{F_\mathrm{i}+N_\mathrm{f}+n+I_\mathrm{f}} \sqrt{[F_\mathrm{i}, F_\mathrm{f}]} \begin{Bmatrix} F_\mathrm{f} & F_\mathrm{i} & n \\ N_\mathrm{i} & N_\mathrm{f} & I_\mathrm{i} \end{Bmatrix} \langle \nu_\mathrm{f}; N_\mathrm{f} || T^{(n)}(\mathbf{M}) || \nu_\mathrm{i}; N_\mathrm{i} \rangle,\end{aligned} \tag{B6}$$

where $[x_1, x_2, \ldots, x_n] = (2x_1 + 1)(2x_1 + 2) \cdots (2x_n + 1)$. This reduction is justified by the fact that the transition operator acts only on the subspace associated with rotational angular momentum and does not modify the nuclear spins.

These two operations lead to

$$\begin{aligned}&\sum_{\mathrm{F_i},(\pm)_\mathrm{i}} \sum_{F_\mathrm{f},(\pm)_\mathrm{f}} \langle \nu_\mathrm{f}; N_\mathrm{f} F_\mathrm{f} m_{\mathrm{F_f}} (\pm)_\mathrm{f} | \mathcal{H}^{\mathrm{HF}} | \nu_\mathrm{f}; N_\mathrm{f} F_\mathrm{f} m_{\mathrm{F_f}} (\pm)_\mathrm{f} \rangle \frac{S_\mathrm{fi}^{\mathrm{HF}}}{S_\mathrm{fi}} \\ &\quad = (-1)^{2(F_i+N_f+n)} \frac{|\langle \nu_\mathrm{f}; N_\mathrm{f} || T^{(n)}(\mathbf{M}) || \nu_\mathrm{i}; N_\mathrm{i} \rangle|^2}{w_I f_n(N_\mathrm{i}, N_\mathrm{f}) \left|\mathbf{M}_\mathrm{fi}^n\right|^2} \sum_{\mathrm{F_i},\mathrm{F_f}(\pm)_\mathrm{f}} [F_\mathrm{i}, F_\mathrm{f}] \langle \nu_\mathrm{f}; N_\mathrm{f} F_\mathrm{f} m_{\mathrm{F_f}} (\pm)_\mathrm{f} | \mathcal{H}^{\mathrm{HF}} | \nu_\mathrm{f}; N_\mathrm{f} F_\mathrm{f} m_{\mathrm{F_f}} (\pm)_\mathrm{f} \rangle \\ &\qquad \times \sum_{I'=|F_\mathrm{f}-N_\mathrm{f}|}^{F_\mathrm{f}+N_\mathrm{f}} a_{I'}^{(\pm)_\mathrm{f}*} \sum_{I''=|F_\mathrm{i}-N_\mathrm{i}|}^{F_\mathrm{i}+N_\mathrm{i}} \delta_{I'I''} (-1)^{I'} \begin{Bmatrix} F_\mathrm{f} & F_\mathrm{i} & n \\ N_\mathrm{i} & N_\mathrm{f} & I'' \end{Bmatrix} \sum_{I'''=|F_\mathrm{f}-N_\mathrm{f}|}^{F_\mathrm{f}+N_\mathrm{f}} a_{I'''}^{(\pm)_\mathrm{f}} \delta_{I''I'''} (-1)^{I'''} \begin{Bmatrix} F_\mathrm{f} & F_\mathrm{i} & n \\ N_\mathrm{i} & N_\mathrm{f} & I'' \end{Bmatrix}.\end{aligned} \tag{B7}$$

The Kronecker deltas reduce the sums over I''' and I''. Using Eq. (A12) in Ref. [41],

$$\frac{\left|\langle \nu_\mathrm{f}; N_\mathrm{f} || T^{(n)}(\mathbf{M}) || \nu_\mathrm{i}; N_\mathrm{i} \rangle\right|^2}{f_n(N_\mathrm{i}, N_\mathrm{f}) \left|\mathbf{M}_\mathrm{fi}^n\right|^2} = 1, \tag{B8}$$

we obtain

$$\begin{aligned}&\sum_{\mathrm{F_i},(\pm)_\mathrm{i}} \sum_{F_\mathrm{f},(\pm)_\mathrm{f}} \langle \nu_\mathrm{f}; N_\mathrm{f} F_\mathrm{f} m_{\mathrm{F_f}} (\pm)_\mathrm{f} | \mathcal{H}^{\mathrm{HF}} | \nu_\mathrm{f}; N_\mathrm{f} F_\mathrm{f} m_{\mathrm{F_f}} (\pm)_\mathrm{f} \rangle \frac{S_\mathrm{fi}^{\mathrm{HF}}}{S_\mathrm{fi}} \\ &\quad = (-1)^{2(F_i+N_f+n)} \frac{1}{w_I} \sum_{\mathrm{F_i},\mathrm{F_f},(\pm)_\mathrm{f}} [F_\mathrm{i}, F_\mathrm{f}] \langle \nu_\mathrm{f}; N_\mathrm{f} F_\mathrm{f} m_{\mathrm{F_f}} (\pm)_\mathrm{f} | \mathcal{H}^{\mathrm{HF}} | \nu_\mathrm{f}; N_\mathrm{f} F_\mathrm{f} m_{\mathrm{F_f}} (\pm)_\mathrm{f} \rangle \sum_{I'=|F_\mathrm{f}-N_\mathrm{f}|}^{F_\mathrm{f}+N_\mathrm{f}} (-1)^{2I'} \left|a_{I'}^{(\pm)_\mathrm{f}}\right|^2 \begin{Bmatrix} F_\mathrm{f} & F_\mathrm{i} & n \\ N_\mathrm{i} & N_\mathrm{f} & I' \end{Bmatrix}^2.\end{aligned} \tag{B9}$$

The sum over F_i involves only the $[F_\mathrm{i}]$ term and the 6-j symbol. This allows us to use the orthogonality of the 6-j symbols,

$$\sum_{F_\mathrm{i}} [F_\mathrm{i}] \begin{Bmatrix} F_\mathrm{f} & F_\mathrm{i} & n \\ N_\mathrm{i} & N_\mathrm{f} & I' \end{Bmatrix}^2 = \frac{1}{[N_\mathrm{f}]}, \tag{B10}$$

which leads to

$$\begin{aligned}&\sum_{\mathrm{F_i},(\pm)_\mathrm{i}} \sum_{F_\mathrm{f},(\pm)_\mathrm{f}} \langle \nu_\mathrm{f}; N_\mathrm{f} F_\mathrm{f} m_{\mathrm{F_f}} (\pm)_\mathrm{f} | \mathcal{H}^{\mathrm{HF}} | \nu_\mathrm{f}; N_\mathrm{f} F_\mathrm{f} m_{\mathrm{F_f}} (\pm)_\mathrm{f} \rangle \frac{S_\mathrm{fi}^{\mathrm{HF}}}{S_\mathrm{fi}} \\ &\quad = (-1)^{2(F_i+N_f+n)} \frac{1}{w_\mathrm{I}[N_\mathrm{f}]} \sum_{F_\mathrm{f},(\pm)_\mathrm{f}} [F_\mathrm{f}] \langle \nu_\mathrm{f}; N_\mathrm{f} F_\mathrm{f} m_{\mathrm{F_f}} (\pm)_\mathrm{f} | \mathcal{H}^{\mathrm{HF}} | \nu_\mathrm{f}; N_\mathrm{f} F_\mathrm{f} m_{\mathrm{F_f}} (\pm)_\mathrm{f} \rangle \sum_{I'=|F_\mathrm{f}-N_\mathrm{f}|}^{F_\mathrm{f}+N_\mathrm{f}} (-1)^{2I'} \left|a_{I'}^{(\pm)_\mathrm{f}}\right|^2.\end{aligned} \tag{B11}$$

Both phase factors can be reduced: N, n, and the sum $F_i + I'$ are always integers. As a consequence, the sum over I' gives 1, according to Eq. (B5),

$$\sum_{\mathrm{F_i},(\pm)_\mathrm{i}} \sum_{F_\mathrm{f},(\pm)_\mathrm{f}} \langle \nu_\mathrm{f}; N_\mathrm{f} F_\mathrm{f} m_{\mathrm{F_f}} (\pm)_\mathrm{f} | \mathcal{H}^{\mathrm{HF}} | \nu_\mathrm{f}; N_\mathrm{f} F_\mathrm{f} m_{\mathrm{F_f}} (\pm)_\mathrm{f} \rangle \frac{S_\mathrm{fi}^{\mathrm{HF}}}{S_\mathrm{fi}} = \frac{1}{w_\mathrm{I}[N_\mathrm{f}]} \sum_{F_\mathrm{f},(\pm)_\mathrm{f}} [F_\mathrm{f}] \langle \nu_\mathrm{f}; N_\mathrm{f} F_\mathrm{f} m_{\mathrm{F_f}} (\pm)_\mathrm{f} | \mathcal{H}^{\mathrm{HF}} | \nu_\mathrm{f}; N_\mathrm{f} F_\mathrm{f} m_{\mathrm{F_f}} (\pm)_\mathrm{f} \rangle. \tag{B12}$$

We recall that in the absence of an external magnetic field, the hyperfine Hamiltonian is diagonal with respect to the projection of the total angular momentum on the space-fixed z axis, m_F. We note that this approach is applicable to experimental techniques

in which the laser field does not considerably shift the hyperfine components (in the extreme case of cavity-enhanced saturation experiments, the dynamical AC Stark shift can be of the order of a few kHz; see Refs. [17,31]). Using

$$\sum_{m_{\mathrm{F_f}}} \langle \nu_\mathrm{f}; N_\mathrm{f} F_\mathrm{f} m_{\mathrm{F_f}} (\pm)_\mathrm{f} | \mathcal{H}^{\mathrm{HF}} | \nu_\mathrm{f}; N_\mathrm{f} F_\mathrm{f} m_{\mathrm{F_f}} (\pm)_\mathrm{f} \rangle = [F_\mathrm{f}] \langle \nu_\mathrm{f}; N_\mathrm{f} F_\mathrm{f} m_{\mathrm{F_f}} (\pm)_\mathrm{f} | \mathcal{H}^{\mathrm{HF}} | \nu_\mathrm{f}; N_\mathrm{f} F_\mathrm{f} m_{\mathrm{F_f}} (\pm)_\mathrm{f} \rangle, \tag{B13}$$

we obtain

$$\sum_{\mathrm{F_i},(\pm)_\mathrm{i}} \sum_{F_\mathrm{f},(\pm)_\mathrm{f}} \langle \nu_\mathrm{f}; N_\mathrm{f} F_\mathrm{f} m_{\mathrm{F_f}} (\pm)_\mathrm{f} | \mathcal{H}^{\mathrm{HF}} | \nu_\mathrm{f}; N_\mathrm{f} F_\mathrm{f} m_{\mathrm{F_f}} (\pm)_\mathrm{f} \rangle \frac{S^{\mathrm{HF}}_{\mathrm{fi}}}{S_{\mathrm{fi}}} = \sum_{F_\mathrm{f}, m_{\mathrm{F_f}}, (\pm)_\mathrm{f}} \frac{\langle \nu_\mathrm{f}; N_\mathrm{f} F_\mathrm{f} m_{\mathrm{F_f}} (\pm)_\mathrm{f} | \mathcal{H}^{\mathrm{HF}} | \nu_\mathrm{f}; N_\mathrm{f} F_\mathrm{f} m_{\mathrm{F_f}} (\pm)_\mathrm{f} \rangle}{w_\mathrm{I}[N_\mathrm{f}]}. \tag{B14}$$

Finally, we transform the matrix element to the coupled basis using Eq. (A4) and summing over the $(\pm)$ labels, given by Eq. (B4), we obtain the first term in Eq. (4). Using exactly the same procedure for the second term in Eq. (B1), we obtain the second term in Eq. (4),

$$\sum_{\mathrm{F_i},(\pm)_\mathrm{i}} \sum_{F_\mathrm{f},(\pm)_\mathrm{f}} \langle \nu_\mathrm{i}; N_\mathrm{i} F_\mathrm{i} m_{\mathrm{F_i}} (\pm)_\mathrm{i} | \mathcal{H}^{\mathrm{HF}} | \nu_\mathrm{i}; N_\mathrm{i} F_\mathrm{i} m_{\mathrm{F_i}} (\pm)_\mathrm{f} \rangle \frac{S^{\mathrm{HF}}_{\mathrm{fi}}}{S_{\mathrm{fi}}} = \sum_{F_\mathrm{i}, m_{\mathrm{F_i}}, I_\mathrm{i}} \frac{\langle \nu_\mathrm{i}; (N_\mathrm{i} I_\mathrm{i}) F_\mathrm{i} m_{\mathrm{F_i}} | \mathcal{H}^{\mathrm{HF}} | \nu_\mathrm{i}; (N_\mathrm{i} I_\mathrm{i}) F_\mathrm{i} m_{\mathrm{F_i}} \rangle}{w_\mathrm{I}[N_\mathrm{i}]}. \tag{B15}$$

2. Heteronuclear case

We express the reduced matrix elements in Eq. (B1) of the transition moment in the coupled basis using Eq. (A5),

$$\begin{aligned}
&\sum_{\mathrm{F_i},(\pm)_\mathrm{i}} \sum_{F_\mathrm{f},(\pm)_\mathrm{f}} \langle \nu_\mathrm{f}; N_\mathrm{f} F_\mathrm{f} m_{\mathrm{F_f}} (\pm)_\mathrm{f} | \mathcal{H}^{\mathrm{HF}} | \nu_\mathrm{f}; N_\mathrm{f} F_\mathrm{f} m_{\mathrm{F_f}} (\pm)_\mathrm{f} \rangle \frac{S^{\mathrm{HF}}_{\mathrm{fi}}}{S_{\mathrm{fi}}} \\
&= \frac{1}{w_I f_n(N_\mathrm{i}, N_\mathrm{f}) |\mathbf{M}^n_{\mathrm{fi}}|^2} \sum_{\mathrm{F_i},(\pm)_\mathrm{i}} \sum_{F_\mathrm{f},(\pm)_\mathrm{f}} \langle \nu_\mathrm{f}; N_\mathrm{f} F_\mathrm{f} m_{\mathrm{F_f}} (\pm)_\mathrm{f} | \mathcal{H}^{\mathrm{HF}} | \nu_\mathrm{f}; N_\mathrm{f} F_\mathrm{f} m_{\mathrm{F_f}} (\pm)_\mathrm{f} \rangle \\
&\quad \times \sum_{F_1'=|F_\mathrm{f}-I_2|}^{F_\mathrm{f}+I_2} a^{(\pm)_\mathrm{f}\,*}_{F_1'} \sum_{F_1''=|F_\mathrm{i}-I_2|}^{F_\mathrm{i}+I_2} a^{(\pm)_\mathrm{i}}_{F_1''} \langle \nu_\mathrm{f}; ((N_\mathrm{f} I_1) F_1' I_2) F_\mathrm{f} || T^{(n)}(\mathbf{M}) || \nu_\mathrm{i}; ((N_\mathrm{i} I_1) F_1'' I_2) F_\mathrm{i} \rangle \\
&\quad \times \sum_{F_1'''=|F_\mathrm{f}-I_2|}^{F_\mathrm{f}+I_2} a^{(\pm)_\mathrm{f}}_{F_1'''} \sum_{F_1''''=|F_\mathrm{i}-I_2|}^{F_\mathrm{i}+I_2} a^{(\pm)_\mathrm{i}\,*}_{F_1''''} \langle \nu_\mathrm{f}; ((N_\mathrm{f} I_1) F_1''' I_2) F_\mathrm{f} || T^{(n)}(\mathbf{M}) || \nu_\mathrm{i}; ((N_\mathrm{i} I_1) F_1'''' I_2) F_\mathrm{i} \rangle^*.
\end{aligned} \tag{B16}$$

We note that the sum over $(\pm)_\mathrm{i}$ involves only the two mixing coefficients. Similar to Eqs. (B4) and (B5), we can formulate the orthogonality relations for the heteronuclear basis,

$$\sum_{(\pm)} a^{(\pm)\,*}_{F_1'} a^{(\pm)}_{F_1''} = \delta_{F_1' F_1''}, \tag{B17}$$

$$\sum_{F_1} a^{(\pm)\,*}_{F_1'} a^{(\pm)}_{F_1'} = \delta_{+-}. \tag{B18}$$

Using Eq. (B17) leads to the reduction of the sum over F_1'''' due to the presence of $\delta_{F_1'' F_1''''}$. Since the transition operator acts only on the subspace of the eigenvectors of $\mathbf{N}^2$, we apply Eq. (B6) twice. Finally, we reduce the $f_n(N_\mathrm{i}, N_\mathrm{f})$ coefficients using Eq. (B8). After applying these three operations, the expression looks as follows:

$$\begin{aligned}
&\sum_{\mathrm{F_i},(\pm)_\mathrm{i}} \sum_{F_\mathrm{f},(\pm)_\mathrm{f}} \langle \nu_\mathrm{f}; N_\mathrm{f} F_\mathrm{f} m_{\mathrm{F_f}} (\pm)_\mathrm{f} | \mathcal{H}^{\mathrm{HF}} | \nu_\mathrm{f}; N_\mathrm{f} F_\mathrm{f} m_{\mathrm{F_f}} (\pm)_\mathrm{f} \rangle \frac{S^{\mathrm{HF}}_{\mathrm{fi}}}{S_{\mathrm{fi}}} \\
&= \frac{1}{w_I} \sum_{\mathrm{F_i},\mathrm{F_f},(\pm)_\mathrm{f}} \langle \nu_\mathrm{f}; N_\mathrm{f} F_\mathrm{f} m_{\mathrm{F_f}} (\pm)_\mathrm{f} | \mathcal{H}^{\mathrm{HF}} | \nu_\mathrm{f}; N_\mathrm{f} F_\mathrm{f} m_{\mathrm{F_f}} (\pm)_\mathrm{f} \rangle \sum_{F_1', F_1'', F_1'''} a^{(\pm)_\mathrm{f}\,*}_{F_1'} a^{(\pm)_\mathrm{f}}_{F_1'''} (-1)^{2(F_\mathrm{i}+2n+I_1+I_2+N_\mathrm{f}+F_1'')} \\
&\quad \times (-1)^{F_1'+F_1'''} [F_\mathrm{i}, F_\mathrm{f}, F_1''] \sqrt{[F_1', F_1''']} \begin{Bmatrix} F_\mathrm{f} & F_\mathrm{i} & n \\ F_1'' & F_1' & I_2 \end{Bmatrix} \begin{Bmatrix} F_1' & F_1'' & n \\ N_\mathrm{i} & N_\mathrm{f} & I_1 \end{Bmatrix} \begin{Bmatrix} F_\mathrm{f} & F_\mathrm{i} & n \\ F_1'' & F_1''' & I_2 \end{Bmatrix} \begin{Bmatrix} F_1''' & F_1'' & n \\ N_\mathrm{i} & N_\mathrm{f} & I_1 \end{Bmatrix}.
\end{aligned} \tag{B19}$$

The first phase factor is reduced immediately: N, n, and the sum $I_1 + F_1$, $I_2 + F$ are always integers. The F_i symbol occurs only in the $[F_\mathrm{i}]$ term and the two 6-j symbols. Using orthonormality of the 6-j symbols,

$$\sum_{F_\mathrm{i}} [F_\mathrm{i}] \begin{Bmatrix} F_\mathrm{f} & F_\mathrm{i} & n \\ F_1'' & F_1' & I_2 \end{Bmatrix} \begin{Bmatrix} F_\mathrm{f} & F_\mathrm{i} & n \\ F_1'' & F_1''' & I_2 \end{Bmatrix} = \frac{\delta_{F_1' F_1'''}}{[F_1']}, \tag{B20}$$

we further simplify the expression for the first distribution moment,

$$\sum_{\mathrm{F_i},(\pm)_\mathrm{i}}\sum_{F_\mathrm{f},(\pm)_\mathrm{f}}\langle \nu_\mathrm{f};N_\mathrm{f}F_\mathrm{f}m_{\mathrm{F_f}}(\pm)_\mathrm{f}|\mathcal{H}^{\mathrm{HF}}|\nu_\mathrm{f};N_\mathrm{f}F_\mathrm{f}m_{\mathrm{F_f}}(\pm)_\mathrm{f}\rangle\frac{S_{\mathrm{fi}}^{\mathrm{HF}}}{S_{\mathrm{fi}}}$$
$$=\frac{1}{w_I}\sum_{\mathrm{F_f},(\pm)_\mathrm{f}}\langle \nu_\mathrm{f};N_\mathrm{f}F_\mathrm{f}m_{\mathrm{F_f}}(\pm)_\mathrm{f}|\mathcal{H}^{\mathrm{HF}}|\nu_\mathrm{f};N_\mathrm{f}F_\mathrm{f}m_{\mathrm{F_f}}(\pm)_\mathrm{f}\rangle\sum_{F_1'}(-1)^{2F_1'}|a_{F_1'}^{(\pm)_\mathrm{f}}|^2[F_\mathrm{f}]\sum_{F_1''}[F_1'']\begin{Bmatrix}F_1' & F_1'' & n\\ N_\mathrm{i} & N_\mathrm{f} & I_1\end{Bmatrix}^2. \tag{B21}$$

The remaining phase factor depends on whether the nuclear spin I_1 is an integer $[(-1)^{2F_1'}=(-1)^{2I_1}=1]$ or a half integer $[(-1)^{2F_1'}=(-1)^{2I_1}=-1]$. We substitute $(-1)^{2F_1'}$ with $(-1)^{2I_1}$, and reduce the sum over F_1'' using Eq. (B20). The remaining sum over F_1', which includes only the mixing coefficient, equals 1, according to Eq. (B18),

$$\sum_{\mathrm{F_i},(\pm)_\mathrm{i}}\sum_{F_\mathrm{f},(\pm)_\mathrm{f}}\langle \nu_\mathrm{f};N_\mathrm{f}F_\mathrm{f}m_{\mathrm{F_f}}(\pm)_\mathrm{f}|\mathcal{H}^{\mathrm{HF}}|\nu_\mathrm{f};N_\mathrm{f}F_\mathrm{f}m_{\mathrm{F_f}}(\pm)_\mathrm{f}\rangle\frac{S_{\mathrm{fi}}^{\mathrm{HF}}}{S_{\mathrm{fi}}}$$
$$=\frac{(-1)^{2I_1}}{w_I[N_f]}\sum_{\mathrm{F_f},(\pm)_\mathrm{f}}[F_\mathrm{f}]\langle \nu_\mathrm{f};N_\mathrm{f}F_\mathrm{f}m_{\mathrm{F_f}}(\pm)_\mathrm{f}|\mathcal{H}^{\mathrm{HF}}|\nu_\mathrm{f};N_\mathrm{f}F_\mathrm{f}m_{\mathrm{F_f}}(\pm)_\mathrm{f}\rangle. \tag{B22}$$

Finally, we use Eq. (B13) and substitute the relation between the eigenvectors of the hyperfine Hamiltonian and the coupled basis vectors from Eq. (A3). This leads to the expected result,

$$\sum_{\mathrm{F_i},(\pm)_\mathrm{i}}\sum_{F_\mathrm{f},(\pm)_\mathrm{f}}\langle \nu_\mathrm{f};N_\mathrm{f}F_\mathrm{f}m_{\mathrm{F_f}}(\pm)_\mathrm{f}|\mathcal{H}^{\mathrm{HF}}|\nu_\mathrm{f};N_\mathrm{f}F_\mathrm{f}m_{\mathrm{F_f}}(\pm)_\mathrm{f}\rangle\frac{S_{\mathrm{fi}}^{\mathrm{HF}}}{S_{\mathrm{fi}}}=(-1)^{2I_1}\sum_{\mathrm{F_f},\mathrm{m_{F_f}}\mathrm{F_{1_f}}}\frac{\langle \nu_\mathrm{f};[(N_\mathrm{f}I_1)F_{1_\mathrm{f}}I_2]F_\mathrm{f}m_{\mathrm{F_f}}|\mathcal{H}^{\mathrm{HF}}|\nu_\mathrm{f};[(N_\mathrm{f}I_1)F_{1_\mathrm{f}}]F_\mathrm{f}m_{\mathrm{F_f}}\rangle}{w_I[N_f]}. \tag{B23}$$

The same mathematical operations can be applied to the second term in Eq. (B1), which results in

$$\sum_{\mathrm{F_i},(\pm)_\mathrm{i}}\sum_{F_\mathrm{f},(\pm)_\mathrm{f}}\langle \nu_\mathrm{i};N_\mathrm{i}F_\mathrm{i}m_{\mathrm{F_i}}(\pm)_\mathrm{i}|\mathcal{H}^{\mathrm{HF}}|\nu_\mathrm{i};N_\mathrm{i}F_\mathrm{i}m_{\mathrm{F_i}}(\pm)_\mathrm{i}\rangle\frac{S_{\mathrm{fi}}^{\mathrm{HF}}}{S_{\mathrm{fi}}}=(-1)^{2I_1}\sum_{\mathrm{F_i},\mathrm{m_{F_i}}\mathrm{F_{1_i}}}\frac{\langle \nu_\mathrm{i};[(N_\mathrm{i}I_1)F_{1_\mathrm{i}}I_2]F_\mathrm{i}m_{\mathrm{F_i}}|\mathcal{H}^{\mathrm{HF}}|\nu_\mathrm{i};[(N_\mathrm{i}I_1)F_{1_\mathrm{i}}]F_\mathrm{i}m_{\mathrm{F_i}}\rangle}{w_I[N_i]}. \tag{B24}$$

Subtracting the two terms leads to an analog of Eq. (4) for heteronuclear molecules,

$$\mathcal{M}_{\mathrm{fi}}{}^{(1)}=\frac{(-1)^{2I_1}}{hw_I}\left(\sum_{\mathrm{F_f},\mathrm{m_{F_f}}\mathrm{F_{1_f}}}\frac{\langle \nu_\mathrm{f};[(N_\mathrm{f}I_1)F_{1_\mathrm{f}}I_2]F_\mathrm{f}m_{\mathrm{F_f}}|\mathcal{H}^{\mathrm{HF}}|\nu_\mathrm{f};[(N_\mathrm{f}I_1)F_{1_\mathrm{f}}]F_\mathrm{f}m_{\mathrm{F_f}}\rangle}{[N_f]}\right.$$
$$\left.-\sum_{\mathrm{F_i},\mathrm{m_{F_i}}\mathrm{F_{1_i}}}\frac{\langle \nu_\mathrm{i};[(N_\mathrm{i}I_1)F_{1_\mathrm{i}}I_2]F_\mathrm{i}m_{\mathrm{F_i}}|\mathcal{H}^{\mathrm{HF}}|\nu_\mathrm{i};[(N_\mathrm{i}I_1)F_{1_\mathrm{i}}]F_\mathrm{i}m_{\mathrm{F_i}}\rangle}{[N_i]}\right). \tag{B25}$$

APPENDIX C: PROOF OF EQ. (8)

We seek a general formula for the trace of the scalar product of two tensors of rank k. Using a formula for matrix elements of the scalar product of two spherical tensors which act on two distinct parts of the coupled basis [47], we obtain

$$\sum_{\nu,j_1,j_2,j,m}\langle \nu;(j_1j_2)jm|T^{(k)}(\mathbf{A})\cdot T^{(k)}(\mathbf{B})|\nu;(j_1j_2)jm\rangle$$
$$=\sum_{\nu,j_1,j_2}(-1)^{j_1+j_2}\left(\sum_j(-1)^j(2j+1)\begin{Bmatrix}j_2 & j_1 & j\\ j_1 & j_2 & k\end{Bmatrix}\right)\langle \nu;j_1||T^{(k)}(\mathbf{A})||\nu;j_1\rangle\langle \nu;j_2||T^{(k)}(\mathbf{B})||\nu;j_2\rangle. \tag{C1}$$

Here, we intentionally distinguish a part of the formula in a bracket. In order to reduce this term, we start with the general orthogonality rule for the 6-j symbols,

$$\sum_{j_3}(2j_3+1)\begin{Bmatrix}j_1 & j_2 & j_3\\ j_4 & j_5 & k\end{Bmatrix}\begin{Bmatrix}j_1 & j_2 & j_3\\ j_4 & j_5 & k'\end{Bmatrix}=\frac{\delta_{kk'}}{2k+1}, \tag{C2}$$

and we put $k'=0$. We recall that in this case, the second 6-j symbol is simplified as follows:

$$\begin{Bmatrix}j_1 & j_2 & j_3\\ j_4 & j_5 & 0\end{Bmatrix}=\frac{\delta_{j_1j_5}\delta_{j_2j_4}}{\sqrt{(2j_1+1)(2j_2+1)}}(-1)^{j_1+j_2+j_3}. \tag{C3}$$

This leads to

$$\sum_{j_3}(-1)^{j_3}(2j_3+1)\begin{Bmatrix} j_1 & j_2 & j_3 \\ j_2 & j_1 & k \end{Bmatrix} = \delta_{k0}(-1)^{-j_1-j_2}\sqrt{(2j_1+1)(2j_2+1)}. \tag{C4}$$

This result, inserted into Eq. (C1) with $j_4 = j_1$, $j_5 = j_2$, and $j_3 = j$, leads to

$$\sum_{\nu,j_1,j_2,j,m}\langle\nu;(j_1j_2)jm|T^{(k)}(\mathbf{A})\cdot T^{(k)}(\mathbf{B})|\nu;(j_1j_2)jm\rangle = \delta_{k0}\sqrt{(2j_1+1)(2j_2+1)}\langle\nu;j_1||T^{(k)}(\mathbf{A})||\nu;j_1\rangle\langle\nu;j_2||T^{(k)}(\mathbf{B})||\nu;j_2\rangle. \tag{C5}$$

APPENDIX D: DERIVATIVE OF THE *N*-GAUSSIAN SPECTRUM

The central frequency of the N-Gaussian spectrum can be determined by calculating the derivative of the sum of N Gaussians, and searching for ν, for which the derivative vanishes. Here, we prove that if the centers of the Gaussians are spread over a narrow range of frequencies, significantly smaller than their widths, the barycenter of the sum of N Gaussians of the same width is given by the formula

$$\nu_{\mathrm{fi}}^{\max} \approx \sum_{\mathrm{HF}} A^{\mathrm{HF}}\nu_{\mathrm{fi}}^{\mathrm{HF}}. \tag{D1}$$

We begin with a simple case of the spectrum which involves two Gaussian functions of different heights, but the same width. The resulting spectrum is

$$f(\nu) = \frac{C}{\sqrt{\pi}\nu_D}e^{-(\nu-a)^2/\nu_D^2} + \frac{C'}{\sqrt{\pi}\nu_D}e^{-(\nu-b)^2/\nu_D^2}. \tag{D2}$$

The two Gaussians are centered around $\nu = a$ and $\nu = b$ and are of C and C' heights, respectively. We slightly modify this equation by introducing the following variables:

$$\begin{aligned} \delta &= \tfrac{1}{2}\ln\frac{C}{C'}, \\ \alpha &= a+b, \\ \beta &= a-b, \\ \xi(\nu) &= e^{\alpha\nu/\nu_D^2-(a^2+b^2)/2\nu_D^2}, \end{aligned} \tag{D3}$$

which allows us to rewrite Eq. (D2) as

$$f(\nu) = \frac{2\sqrt{CC'}}{\sqrt{\pi}\nu_D}e^{-\nu^2/\nu_D^2}\xi(\nu)\cosh\left[\frac{\beta}{\nu_D^2}(\nu-\alpha)+\delta\right]. \tag{D4}$$

The extrema of the spectrum occur at ν for which $f'(\nu) = 0$. This leads to a nonlinear equation on ν,

$$\nu = \frac{\beta}{2}\tanh\left[\frac{\beta}{\nu_D^2}(\nu-\alpha)+\delta\right]+\frac{\alpha}{2}. \tag{D5}$$

An approximate solution can be found using Taylor expansion. First, we use the formula for the sum of arguments of the hyperbolic tangent,

$$\tanh(a+b) = \frac{\tanh(a)+\tanh(b)}{1+\tanh(a)\tanh(b)}, \tag{D6}$$

we rewrite the resulting equation using a new variable, $x = \frac{\beta}{\nu_D^2}(\nu-\alpha)$, and we expand the right-hand side of Eq. (D5) for $x \ll 1$, keeping only the terms that are linear in x,

$$\nu^{\max} \approx \frac{\beta}{2}\frac{\tanh(\delta)+\frac{\beta}{\nu_D^2}(\nu-\alpha)}{1+\tanh(\delta)\frac{\beta}{\nu_D^2}(\nu-\alpha)}+\frac{\alpha}{2}. \tag{D7}$$

The remaining hyperbolic tangent is simply

$$\tanh\delta = \frac{C-C'}{C+C'}. \tag{D8}$$

If $x \ll 1$, then $\frac{C-C'}{C+C'}x \ll 1$ too. Thus, in the next step, we expand the denominator and we neglect all terms smaller than the linear term on the right-hand side of the equation. This leads to

$$\nu^{\max} \approx \frac{\frac{1}{2}\frac{\beta(C-C')+\alpha(C+C')}{C+C'} - \frac{\alpha\beta}{\nu_D^2}\left(1-\frac{(C-C')^2}{(C+C')^2}\right)}{1-\frac{\beta^2}{2\nu_D^2}\left(1-\frac{(C-C')^2}{(C+C')^2}\right)}, \tag{D9}$$

which is drastically simplified if $\beta/\nu_D \ll 1$. Substituting a and b for α and β from Eq. (D3) results in

$$\nu^{\max} \approx a\bar{C}+b\bar{C}', \tag{D10}$$

where $\bar{C} = C/(C+C')$ and $\bar{C}' = C'/(C+C')$ are relative intensities of the two components. This result resembles the form anticipated in Eq. (D1). We thus have provided a position of the maximum of Eq. (D2) for $\beta/\nu_D \ll 1$.

Additionally, we can show that if $a/\nu_D \ll 1$ and $b/\nu_D \ll 1$, the general formula from Eq. (D2) is simplified into a single Gaussian, centered at $\nu^{\max}$ with the height of $C+C'$. We approximate the exponents involving a and b as $e^x \approx 1+x$ in Eq. (D2), and we keep only the terms that are linear in a/ν_D and b/ν_D. This leads to

$$f(\nu) \approx \frac{(C+C')}{\sqrt{\pi}\nu_D}e^{-\nu^2/\nu_D^2}\left(1+2\frac{\nu}{\nu_D}\frac{aC+bC'}{C+C'}\right), \tag{D11}$$

which corresponds to the approximation of

$$f(\nu) = \frac{(C+C')}{\sqrt{\pi}\nu_D}e^{-(\nu-\nu^{\max})^2/\nu_D^2} \tag{D12}$$

for $\nu^{\max}/\nu_D \ll 1$. We write, symbolically, that

$$f(\nu) = f(\nu;a,C)+f(\nu;b,C') \approx f(\nu;\nu^{\max(2)},C^{(2)}), \tag{D13}$$

which means that the sum of two Gaussians of the same width, centered around a and b, leads to another Gaussian, centered around $\nu^{\max} = \nu^{\max(2)}$ [the (2) superscript denotes the number of summed Gaussians], given by Eq. (D10). The resulting

profile is of the height which is the sum of the two Gaussian functions, $C^{(2)} = C + C'$.

We apply the same procedure to another Gaussian, centered around c and of the height given by C''. Using the same arguments as in the two-Gaussian case, the central frequency of the profile resulting from summing *three* Gaussians is given as

$$\nu^{\max\,(3)} \approx a\bar{C} + b\bar{C}' + c\bar{C}''. \tag{D14}$$

This iterative approach can be used for the N-Gaussian case. If all conditions introduced throughout the derivation remain fulfilled, the central frequency of the set of N-Gaussian functions, $f(\nu; \nu_{0i}, C_i)$ is given by

$$\nu^{\max\,(\mathrm{N})} \approx \sum_{i=1}^{N} \nu_{0i}\bar{C}_i. \tag{D15}$$

Thus, the maximum of the profile resulting from summing N-Gaussian functions involves the first moment, defined in Sec. II. If all Gaussians fulfill the condition,

$$\sum_{i=1}^{N} \nu_{0i}\bar{C}_i = 0, \tag{D16}$$

the maximum of the resulting profile corresponds to the zero frequency.

[1] S. Alighanbari, G. S. Giri, F. L. Constantin, V. I. Korobov, and S. Schiller, Precise test of quantum electrodynamics and determination of fundamental constants with HD^+ ions, Nature (London) **581**, 152 (2020).

[2] S. Patra, M. Germann, J.-P. Karr, M. Haidar, L. Hilico, V. I. Korobov, F. M. J. Cozijn, K. S. E. Eikema, W. Ubachs, and J. C. J. Koelemeij, Proton-electron mass ratio from laser spectroscopy of HD^+ at the part-per-trillion level, Science **369**, 1238 (2020).

[3] A. Beyer, L. Maisenbacher, A. Matveev, R. Pohl, K. Khabarova, A. Grinin, T. Lamour, D. C. Yost, T. W. Hänsch, N. Kolachevsky, and T. Udem, The Rydberg constant and proton size from atomic hydrogen, Science **358**, 79 (2017).

[4] R. Pohl, A. Antognini, F. Nez, F. D. Amaro, F. Biraben, J. M. R. Cardoso, D. S. Covita, A. Dax, S. Dhawan, L. M. P. Fernandes *et al.*, The size of the proton, Nature (London) **466**, 213 (2010).

[5] W. Ubachs, J. Koelemeij, K. Eikema, and E. Salumbides, Physics beyond the Standard Model from hydrogen spectroscopy, J. Mol. Spectrosc. **320**, 1 (2016).

[6] M. S. Safronova, D. Budker, D. DeMille, Derek F. Jackson Kimball, A. Derevianko, and C. W. Clark, Search for new physics with atoms and molecules, Rev. Mod. Phys. **90**, 025008 (2018).

[7] L. Wolniewicz, I. Simbotin, and A. Dalgarno, Quadrupole transition probabilities for the excited rovibrational states of H_2, Astrophys. J., Suppl. Ser. **115**, 293 (1998).

[8] A. Campargue, S. Kassi, K. Pachucki, and J. Komasa, The absorption spectrum of H_2: CRDS measurements of the (2-0) band, review of the literature data and accurate *ab initio* line list up to 35000 cm^{-1}, Phys. Chem. Chem. Phys. **14**, 802 (2012).

[9] K. Pachucki and J. Komasa, Magnetic dipole transitions in the hydrogen molecule, Phys. Rev. A **83**, 032501 (2011).

[10] E. Roueff, H. Abgrall, P. Czachorowski, K. Pachucki, M. Puchalski, and J. Komasa, The full infrared spectrum of molecular hydrogen, Astron. Astrophys. **630**, A58 (2019).

[11] A. Fast and S. A. Meek, Sub-ppb Measurement of a Fundamental Band Rovibrational Transition in HD, Phys. Rev. Lett. **125**, 023001 (2020).

[12] M. L. Diouf, F. M. J. Cozijn, K.-F. Lai, E. J. Salumbides, and W. Ubachs, Lamb-peak spectrum of the HD (2-0) P(1) line, Phys. Rev. Res. **2**, 023209 (2020).

[13] T.-P. Hua, Y. Sun, and S.-M. Hu, Dispersion-like lineshape observed in cavity-enhanced saturation spectroscopy of HD at 1.4 μm, Opt. Lett. **45**, 4863 (2020).

[14] M. Zaborowski, M. Słowiński, K. Stankiewicz, F. Thibault, A. Cygan, H. Jóźwiak, G. Kowzan, P. Masłowski, A. Nishiyama, N. Stolarczyk, S. Wójtewicz, R. Ciuryło, D. Lisak, and P. Wcisło, Ultrahigh finesse cavity-enhanced spectroscopy for accurate tests of quantum electrodynamics for molecules, Opt. Lett. **45**, 1603 (2020).

[15] A. Castrillo, E. Fasci, and L. Gianfrani, Doppler-limited precision spectroscopy of HD at 1.4 μm: An improved determination of the R(1) center frequency, Phys. Rev. A **103**, 022828 (2021).

[16] A. Fast and S. A. Meek, Precise measurement of the $D_2S_1(0)$ vibrational transition frequency, Mol. Phys. **120**, e1999520 (2021).

[17] H. Jóźwiak and P. Wcisło, Magic wavelength for a rovibrational transition in molecular hydrogen, Sci. Rep. **12**, 14529 (2022).

[18] P. Dupré, Hyperfine transitions in the first overtone mode of hydrogen deuteride, Phys. Rev. A **101**, 022504 (2020).

[19] H. Jóźwiak, H. Cybulski, and P. Wcisło, Positions and intensities of hyperfine components of all rovibrational dipole lines in the HD molecule, J. Quant. Spectrosc. Radiat. Transfer **253**, 107171 (2020).

[20] H. Jóźwiak, H. Cybulski, and P. Wcisło, Hyperfine components of all rovibrational quadrupole transitions in the H_2 and D_2 molecules, J. Quant. Spectrosc. Radiat. Transfer **253**, 107186 (2020).

[21] J. Komasa, M. Puchalski, and K. Pachucki, Hyperfine structure in the HD molecule, Phys. Rev. A **102**, 012814 (2020).

[22] H. Jóźwiak, H. Cybulski, and P. Wcisło, Hyperfine structure of quadrupole rovibrational transitions in tritium-bearing hydrogen isotopologues, J. Quant. Spectrosc. Radiat. Transfer **256**, 107255 (2020).

[23] M. Puchalski, J. Komasa, and K. Pachucki, Hyperfine Structure of the First Rotational Level in H_2, D_2 and HD Molecules and the Deuteron Quadrupole Moment, Phys. Rev. Lett. **125**, 253001 (2020).

[24] H. Jóźwiak, H. Cybulski, and P. Wcisło, Hyperfine components of rovibrational dipole transitions in HT and DT, J. Quant. Spectrosc. Radiat. Transfer **270**, 107662 (2021).

[25] H. Jóźwiak, H. Cybulski, and P. Wcisło, Hyperfine components of rovibrational quadrupole transitions in HD, J. Quant. Spectrosc. Radiat. Transfer **272**, 107753 (2021).

[26] G. D. Dickenson, M. L. Niu, E. J. Salumbides, J. Komasa, K. S. E. Eikema, K. Pachucki, and W. Ubachs, Fundamental Vibration of Molecular Hydrogen, Phys. Rev. Lett. **110**, 193601 (2013).

[27] M. Niu, E. Salumbides, G. Dickenson, K. Eikema, and W. Ubachs, Precision spectroscopy of the $X^1\Sigma_{g+}$, $v = 0 \rightarrow 1(J = 0 - 2)$ rovibrational splittings in H_2, HD and D_2, J. Mol. Spectrosc. **300**, 44 (2014).

[28] D. Mondelain, S. Kassi, T. Sala, D. Romanini, D. Gatti, and A. Campargue, Sub-MHz accuracy measurement of the S(2) 2–0 transition frequency of D_2 by Comb-Assisted Cavity Ring Down spectroscopy, J. Mol. Spectrosc. **326**, 5 (2016).

[29] P. Wcisło, F. Thibault, M. Zaborowski, S. Wójtewicz, A. Cygan, G. Kowzan, P. Masłowski, J. Komasa, M. Puchalski, K. Pachucki, R. Ciuryło, and D. Lisak, Accurate deuterium spectroscopy for fundamental studies, J. Quant. Spectrosc. Radiat. Transfer **213**, 41 (2018).

[30] L.-G. Tao, A.-W. Liu, K. Pachucki, J. Komasa, Y. R. Sun, J. Wang, and S.-M. Hu, Toward a Determination of the Proton-Electron Mass Ratio from the Lamb-Dip Measurement of HD, Phys. Rev. Lett. **120**, 153001 (2018).

[31] F. M. J. Cozijn, P. Dupré, E. J. Salumbides, K. S. E. Eikema, and W. Ubachs, Sub-Doppler Frequency Metrology in HD for Tests of Fundamental Physics, Phys. Rev. Lett. **120**, 153002 (2018).

[32] E. Fasci, A. Castrillo, H. Dinesan, S. Gravina, L. Moretti, and L. Gianfrani, Precision spectroscopy of HD at 1.38 μm, Phys. Rev. A **98**, 022516 (2018).

[33] M. Beyer, N. Hölsch, J. Hussels, C.-F. Cheng, E. J. Salumbides, K. S. E. Eikema, W. Ubachs, C. Jungen, and F. Merkt, Determination of the Interval Between the Ground States of Para- and Ortho-H_2, Phys. Rev. Lett. **123**, 163002 (2019).

[34] M. L. Diouf, F. M. J. Cozijn, B. Darquié, E. J. Salumbides, and W. Ubachs, Lamb-dips and lamb-peaks in the saturation spectrum of HD, Opt. Lett. **44**, 4733 (2019).

[35] D. Mondelain, S. Kassi, and A. Campargue, Transition frequencies in the (2-0) band of D_2 with MHz accuracy, J. Quant. Spectrosc. Radiat. Transfer **253**, 107020 (2020).

[36] S. Wójtewicz, R. Gotti, D. Gatti, M. Lamperti, P. Laporta, H. Jóźwiak, F. Thibault, P. Wcisło, and M. Marangoni, Accurate deuterium spectroscopy and comparison with *ab initio* calculations, Phys. Rev. A **101**, 052504 (2020).

[37] J. Liu, E. J. Salumbides, U. Hollenstein, J. C. J. Koelemeij, K. S. E. Eikema, W. Ubachs, and F. Merkt, Determination of the ionization and dissociation energies of the hydrogen molecule, J. Chem. Phys. **130**, 174306 (2009).

[38] C.-F. Cheng, J. Hussels, M. Niu, H. L. Bethlem, K. S. E. Eikema, E. J. Salumbides, W. Ubachs, M. Beyer, N. Hölsch, J. A. Agner, F. Merkt, L.-G. Tao, S.-M. Hu, and C. Jungen, Dissociation Energy of the Hydrogen Molecule at 10^{-9} Accuracy, Phys. Rev. Lett. **121**, 013001 (2018).

[39] N. Hölsch, M. Beyer, E. J. Salumbides, K. S. E. Eikema, W. Ubachs, C. Jungen, and F. Merkt, Benchmarking Theory with an Improved Measurement of the Ionization and Dissociation Energies of H_2, Phys. Rev. Lett. **122**, 103002 (2019).

[40] S. Kassi, C. Lauzin, J. Chaillot, and A. Campargue, The (2-0) R(0) and R(1) transition frequencies of HD determined to a 10^{-10} relative accuracy by Doppler spectroscopy at 80 K, Phys. Chem. Chem. Phys. **24**, 23164 (2022).

[41] H. Jóźwiak and P. Wcisło, Relative intensities of hyperfine components of rovibrational transitions in molecular hydrogen, Phys. Rev. A **105**, 062812 (2022).

[42] This is not the case for *para*-H_2 and *para*-T_2, which do not exhibit hyperfine structure, since the total nuclear spin is 0.

[43] U. Fano and G. Racah, *Irreducible Tensorial Sets*, Cambridge Molecular Science (Academic Press, Cambridge, MA, 1959).

[44] R. L. Cook and F. C. D. Lucia, Application of the theory of irreducible tensor operators to molecular hyperfine structure, Am. J. Phys. **39**, 1433 (1971).

[45] E. Arimondo, M. Inguscio, and P. Violino, Experimental determinations of the hyperfine structure in the alkali atoms, Rev. Mod. Phys. **49**, 31 (1977).

[46] M. Broyer, J. Vigué, and J. Lehmann, Effective hyperfine Hamiltonian in homonuclear diatomic molecules. Application to the B state of molecular iodine, J. Phys. France **39**, 591 (1978).

[47] J. M. Brown and A. Carrington, *Rotational Spectroscopy of Diatomic Molecules*, Cambridge Molecular Science (Cambridge University Press, Cambridge, 2003).

[48] G. Herzberg and L. Howe, The Lyman bands of molecular hydrogen, Can. J. Phys. **37**, 636 (1959).

[49] J.-M. Hartmann, C. Boulet, and D. Robert, *Collisional Effects on Molecular Spectra* (Elsevier, Amsterdam, 2021).

[50] P. Wcisło, I. Gordon, H. Tran, Y. Tan, S.-M. Hu, A. Campargue, S. Kassi, D. Romanini, C. Hill, R. Kochanov, and L. Rothman, The implementation of non-Voigt line profiles in the HITRAN database: H_2 case study, J. Quant. Spectrosc. Radiat. Transfer **177**, 75 (2016).

[51] P. Wcisło, I. E. Gordon, C.-F. Cheng, S.-M. Hu, and R. Ciuryło, Collision-induced line-shape effects limiting the accuracy in Doppler-limited spectroscopy of H_2, Phys. Rev. A **93**, 022501 (2016).

[52] G. Buffa and O. Tarrini, Hyperfine effects on spectral line shape. II. The case DCO^+–He, J. Chem. Phys. **134**, 174310 (2011).

[53] M. Lamperti, L. Rutkowski, D. Ronchetti, D. Gatti, R. Gotti, G. Cerullo, F. Thibault, H. Jóźwiak, S. Wójtewicz, P. Masłowski, P. Wcisło, D. Polli, and M. Marangoni, Stimulated-Raman-scattering metrology, arXiv:2207.03998.

[54] G. Buffa, A. Di Lieto, P. Minguzzi, O. Tarrini, and M. Tonelli, Nuclear-quadrupole effects in the pressure broadening of molecular lines, Phys. Rev. A **37**, 3790 (1988).

[55] S. Belli, G. Buffa, and O. Tarrini, Collisional coupling between hyperfine and Stark components of molecular spectra, Phys. Rev. A **55**, 183 (1997).

[56] S. Green, Effect of nuclear hyperfine structure on microwave spectral pressure broadening, J. Chem. Phys. **88**, 7331 (1988).

[57] G. Buffa and O. Tarrini, Hyperfine effects on collisional line shape. I. A self-consistent set of equations, J. Chem. Phys. **134**, 174309 (2011).

[58] M. Słowiński, F. Thibault, Y. Tan, J. Wang, A.-W. Liu, S.-M. Hu, S. Kassi, A. Campargue, M. Konefał, H. Jóźwiak *et al.*, H_2-He collisions: *Ab initio* theory meets cavity-enhanced spectra, Phys. Rev. A **101**, 052705 (2020).

[59] P.-M. Flaud, J. Orphal, C. Boulet, and J.-M. Hartmann, Measurements and analysis of collisional line-mixing within nuclear hyperfine components of helium broadened HI lines, J. Mol. Spectrosc. **235**, 149 (2006).

[60] Wroclaw Centre for Networking and Supercomputing, https://wcss.pl.

[61] J. Muenter and W. Klemperer, Hyperfine structure constants of HF and DF, J. Chem. Phys. **52**, 6033 (1970).

[62] G. Cazzoli, L. Dore, C. Puzzarini, and S. Beninati, Millimeter- and submillimeter-wave spectrum of $C^{17}O$. Rotational hyperfine structure analyzed using the Lamb-dip technique, Phys. Chem. Chem. Phys. **4**, 3575 (2002).

[63] G. Klapper, L. Surin, F. Lewen, H. S. Müller, I. Pak, and G. Winnewisser, Laboratory precision measurements of the rotational spectrum of $^{12}C^{17}O$ and $^{13}C^{17}O$, Astrophys. J. **582**, 262 (2003).

[64] G. Cazzoli and C. Puzzarini, Hyperfine structure of the $J = 1 \leftarrow 0$ transition of $H^{35}Cl$ and $H^{37}Cl$: Improved ground state parameters, J. Mol. Spectrosc. **226**, 161 (2004).

[65] E. W. Kaiser, Dipole moment and hyperfine parameters of $H^{35}Cl$ and $D^{35}Cl$, J. Chem. Phys. **53**, 1686 (1970).

[66] D. W. Johnson and N. F. Ramsey, Stark hyperfine structure of hydrogen bromide, J. Chem. Phys. **67**, 941 (1977).

[67] F. Van Dijk and A. Dymanus, Hyperfine structure of the rotational spectrum of HI in the submillimeter region, Chem. Phys. Lett. **2**, 235 (1968).

[68] F. C. De Lucia, P. Helminger, and W. Gordy, Submillimeter-wave spectra and equilibrium structures of the hydrogen halides, Phys. Rev. A **3**, 1849 (1971).

[69] A. O. G. Wallis and R. V. Krems, Magnetic Feshbach resonances in collisions of nonmagnetic closed-shell $^1\Sigma$ molecules, Phys. Rev. A **89**, 032716 (2014).